UNIVERSIDADE FEDERAL DE SÃO CARLOS
Centro de Ciências Exatas e de Tecnologia
Programa de Pós Graduação em Física

Marcos A. G. dos Santos Filho

Incompressible Energy Spectrum in Atomic Bose–Einstein Condensates:

A Weak Wave Turbulence Theory Approach

São Carlos, SP
September, 2022

Incompressible Energy Spectrum in Atomic Bose–Einstein Condensates:

A Weak Wave Turbulence Theory Approach

Trabalho apresentado ao Programa de Pós-Graduação em Física da Universidade Federal de São Carlos como parte dos pré-requisitos para obtenção do titulo de Doutor em Ciências.
Area de Concentração: Física

Marcos A. G. dos Santos Filho

Supervisor:
Prof. Dr. Francisco Ednilson A. dos Santos

September, 2022

UNIVERSIDADE FEDERAL DE SÃO CARLOS

Centro de Ciências Exatas e de Tecnologia
Programa de Pós-Graduação em Física

Folha de Aprovação

Defesa de Tese de Doutorado do candidato Marcos Alberto Gonçalves dos Santos Filho, realizada em 25/08/2022.

Comissão Julgadora:

Prof. Dr. Francisco Ednilson Alves dos Santos (UFSCar)

Prof. Dr. Emanuel Fernandes de Lima (UFSCar)

Prof. Dr. Raul Celistrino Teixeira (UFSCar)

Prof. Dr. Emanuel Alves de Lima Henn (USP)

Profa. Dra. Mônica Adrioli Caracanhas Santarelli (USP)

O Relatório de Defesa assinado pelos membros da Comissão Julgadora encontra-se arquivado junto ao Programa de Pós-Graduação em Física.

To my father, in loving memory.

Acknowledgments

I'm eternally grateful to my advisor, Prof. Francisco Ednilson A. dos Santos, for all the patience and the wisdom shared during this journey. I'm also thankful to my group colleagues, Renan and Ricardo, who both became irreplaceable friends. The discussions at our office were essential not only for the development of this project but also to my personal growth as a researcher.

I'd like to express my gratitude to my family, especially my parents Marinei and Marcos[†] who were always proud and a constant source of support through the more difficult times.

I would be remiss if I didn't mention my friends, Paola, Diego, Natália, Tati, Eduardo, Marina, Gustavo, Caique, Carol, Paulo, Dani, Dani, Ana, Maju, Jeferson and Murilo. Some are new, some are old but all have provided company, wisdom and plenty of laughs.

This study was financially supported by the Conselho Nacional de Desenvolvimento Científico e Tecnológico (CNPq) through grant Doutorado - GD process number: 141249/2018-8.

Abstract

Bose–Einstein condensates with their superfluidity property provide an interesting parallel to classical fluids. Due to the Kolmogorov spectrum of homogeneous turbulence the statistics of the incompressible velocity field is of great interest, but in superfluids obtaining quantities such as the statistics of the velocity field from the macroscopic wavefunction turns out be a complicated task; therefore, most of the work up to now has been numerical in nature. We made use of the Weak Wave Turbulence (WWT) theory, which provides the statistics of the macroscopic wavefunction, to obtain the statistics of the velocity field, which allowed us to produce a semi analytical procedure for extracting the incompressible energy spectrum in the WWT regime. This is done by introducing an auxiliary wavefunction that preserves the relevant statistical and hydrodynamical properties of the condensate but with a homogeneous density thus allowing for a simpler description of the velocity field.

Resumo

Condensados de Bose–Einstein apresentam um paralelo interessante a fluídos clássicos devido a sua propriedade de superfluidez. A estatística da parte incompressível do campo de velocidade é de grande interesse devido ao espectro de Kolmogorov presente em turbulência homogênea, porém em superfluídos quantidades relacionadas a estatística do campo de velocidades podem ser complicadas de obter e a maior parte dos trabalhos até o momento tem sido de natureza numérica. Nós nos aproveitamos da teoria de turbulência de ondas fracamente interagente, a qual descreve a estatística da função de onda macroscópica, para obter a estatística do campo de velocidades. Essa abordagem nos permitiu desenvolver um procedimento semi analítico para extrair o espectro de energia incompressível no regime de turbulência de ondas. Este procedimento consiste em introduzir uma função de onda auxiliar que preserva as propriedades estatísticas e hidrodinâmicas relevantes e possui um perfil de densidade homogêneo, permitindo então uma descrição simplificado do campo de velocidades.

List of Figures

List of Acronyms

BEC Bose–Einstein Condensate. 2, 5, 11, 21, 33, 42, 43

CNPq Conselho Nacional de Desenvolvimento Científico e Tecnológico. v

GPE Gross–Pitaevskii Equation. 8, 16, 21–23, 33, 34, 43

JILA Joint Institute for Laboratory Astrophysics. 2

K41 Kolmogorov-Obukhov Spectrum. 2, 15, 20, 33, 42

MIT Massachusetts Institute of Technology. 2

RPA Random Phase and Amplitude. 24, 25, 27, 34

WWT Weak Wave Turbulence. vii, 2, 3, 21, 23, 31, 33, 34, 39–41, 43

Contents

Chapter 1

Introduction

Below a critical temperature liquid ^4He behaves in an unfamiliar manner. This was first observed independently in the late 1930s by Kapitza [1] and Allen and Misener [2] by managing to cool liquid helium below a temperature of $T = 2.17K$. Below this temperature the fluid could flow through extremely narrow channels without any measurable resistance, seemly like an ideal fluid with zero viscosity, which led Kapitza to refer to it as a *superfluid* [3].

In an experiment using oscillating discs Keesom and Macwood [4] verified that while the viscosity seemed to be positively dependent on the temperature, there was still a finite measurable viscosity at temperatures below the lambda point. This was followed with the idea of a two component fluid by Tisza [5] and later by Landau [6]. The two components consist of a normal component and a superfluid component; the superfluid flows without viscosity while the normal component behaves as a classical fluid. London [7] proposed that the superfluid component could be understood as a manifestation of Bose–Einstein condensation. The results of Keesom and Macwood experiment could be understood as the discs not being able to avoid partial interaction with the normal fluid.

These ideas would be more formally defined throughout the next decades especially with the formalization of a macroscopic wavefunction and the idealization of quantized vortices by Feynman [8], Onsager [9], and Penrose and Onsager [10].

The following early experimental evidence of quantized circulation by Vinen [11] further served to cement superfluidity as a quantum phenomenon, particularly a macroscopic observable quantum effect.

1.1 Bose–Einstein Condensation

What is today called Bose–Einstein condensation was first postulated by Einstein [12] when applying the recently developed Bose statistics to a monatomic non-interacting gas. Einstein

would find something quite puzzling, below a certain temperature it appeared that identical particles seemed to be able to occupy the same state which he noted to be paradoxical [13]. The superfluid discovery and the aforementioned connection with what then was already being called Bose–Einstein condensation would for a long time be the strongest evidence of this phenomenon.

But a liquid, like superfluid helium, is quite far from the ideal non-interacting gas envisioned by Einstein. In the decades followed by the superfluid discovery the theory of Bose–Einstein Condensate (BEC) was expanded by Bogolubov [14], Gross [15], and Pitaevskii [16], among others.

The experimental realization of a "true" atomic BEC would come approximately 70 years after Einstein observations. In 1995 a team at the Joint Institute for Laboratory Astrophysics (JILA) managed to cool a gas of rubidium to an unprecedented temperature of $20nK$ [17], this was followed closely by a group at the Massachusetts Institute of Technology (MIT) which achieved similar results with a gas of sodium [18]. These results were made possible by advances in trapping techniques that enabled the combination of two cooling strategies, laser cooling and evaporative cooling.

Since the realization of the first atomic BEC the field has seen a steady growth and only a few years later we would see experimental observation of quantized vortices [19, 20, 21], the use of condensates as atomic interferometers [22] and as possible analogues for the study of black hole radiation [23]. Today the production of condensates are an everyday occurrence in Laboratories throughout the world and recently even in orbit [24], which opens up the door for more exploration in the behaviour of quantum systems in a microgravity environment.

Another field of interest that developed in parallel throughout the years was the field of quantum turbulence. The idea of quantized vortices make superfluids attractive for the study of turbulence since it offers simpler structures to deal with. Classical turbulence is characterized by continuous three-dimensional vortex structures and largely non-linear behaviour. In spite of that the well known Kolmogorov-Obukhov Spectrum (K41) and the Richardson cascade mechanism serve as signatures for well-developed turbulence systems [25]. The first experimental evidence of the presence of Kolmogorov like behaviour in superfluid helium was made by Maurer and Tabeling [26] and although no Kolmogorov cascade has been observed in atomic BEC, only vortex tangles like in [27], numerical works have demonstrated that it should be possible [28, 29, 30].

In this thesis we extend the current knowledge of quantum turbulence by providing a method to obtain an analytical prediction for the incompressible energy spectrum. The method relies on the so called Weak Wave Turbulence (WWT) theory which is similar to general turbulence but instead of dealing with the non-linearity of the vortex interaction it concentrates on the non-linear behaviour of the waves [31]. Its limitation is that is only well-defined for weakly interacting systems limiting its application to atomic BEC [32]. We employ an auxiliary wavefunction to

show that WWT and hydrodynamical turbulence are connected by demonstrating that the velocity field statistics is dependent on the wave statistics.

Chapter 2

Atomic Bose–Einstein Condensate

Dilute gases

Dilute gases have much lower volumetric density when compared with other types of matter such as liquids, solids or non dilute gases. If we call the average diameter of an atom in the gas σ and the number density[1] n then we say that a gas is dilute if $n\sigma^3 \ll 1$. This definition implies that the average spacing between the atoms is large in comparison with the average diameter of the atomic species, which in turn means that the gas behaves to great approximation as an ideal gas [33].

The experimental realization of a BEC in dilute gases was achieved through the combination of laser and evaporative cooling techniques, leading to two separate groups managing to cool a cloud of atoms below the necessary critical temperatures and to observe a macroscopic occupation of the system's ground state in 1995 [17, 18].

In the interest of developing some intuition about the scale of the physical quantities let us make some naive approximations using dimensional analysis. The relevant quantities are the reduced Planck constant $\hbar$, the number density n, the atomic mass m and the Boltzman constant κ_B, then we have

$$T_C = f(\hbar, n, m, \kappa_B) \Rightarrow \begin{array}{l} [T_C] = [\hbar]^a [n]^b [m]^c [\kappa]^d \\ [\theta] = \left([M][L]^2[T]^{-1}\right)^a [L]^{-3b} [M]^c \left([M][L]^2[T]^{-2}[\theta]^{-1}\right)^d \end{array}$$

with $[L]$, $[M]$, $[T]$, $[\theta]$ representing the irreducible unities of length, mass, time and temperature,

[1] Number of atoms per unit volume.

respectively. Now, solving the resulting linear system

$$\begin{aligned} 2a - 3b + 2d &= 0 \\ a + c + d &= 0 \\ -a - 2d &= 0 \\ -d &= 1 \end{aligned}$$

we find that $a = 2$, $b = \frac{2}{3}$, $c = -1$, $d = -1$, therefore

$$T_C = \alpha \frac{\hbar^2 n^{2/3}}{m\kappa_B} \tag{2.1}$$

with α being a dimensionless proportionality constant dependent on the geometry and dimensionality of the system. For a uniform gas in a three-dimensional box, $\alpha \simeq 3.31$ [34].

2.1 Bose–Einstein Condensation: The Gross–Pitaevskii Model

What is generally implied when the term Bose–Einstein condensation is used is the macroscopic occupation of the system's ground state. One simple way of formalizing this idea is by introducing the condensate fraction,

$$F_c = \frac{N_0}{N},$$

where N_0 represents the number of particles in the ground state and N the total number of particles. We follow by establishing the *thermodynamic limit* as being related to the density of the system remaining finite as the size, V, and the number of particles grows to infinity:

$$\lim_{N,V\to\infty} \frac{N}{V} = \text{const.} \tag{2.2}$$

Then a criterion for condensation can be formulated as

$$\lim_{N\to\infty} F_c > 0 \tag{2.3}$$

where the limit in (2.2) is assumed to exist. This is sometimes called the Einstein Criterion for condensation [35].

In the following discussion we will assume a weakly interacting Bose gas at zero temperature with $F_c = 1$, that is, all of its particles are in the ground state.

In such a system the following hypothesis can be assumed:

- Since all the N atoms are in the same state the system can be described by the symmetrized state (2.4)

$$\Psi\left(\mathbf{r}_1, \mathbf{r}_2, \ldots, \mathbf{r}_N\right) = \prod_{i=1}^{i=N} \psi_s(\mathbf{r}_i), \tag{2.4}$$

  with $\Psi\left(\mathbf{r}\right)$ representing the quantum state of the system and $\psi_s\left(\mathbf{r}_i\right)$ the single state of the i-th atom.

- In such a low temperature system only $s-$wave interactions need to be accounted for, in this way the inter atomic interactions can be taken to be contact interactions with interaction parameter

$$g = \frac{4\pi\hbar^2 a}{m}, \tag{2.5}$$

  where a is the s-wave scattering length of the system, $\hbar$ the reduced Planck constant and m the atomic species mass.

- The single atom states are normalized:

$$\int \mathrm{d}^n r \left|\psi_s(\mathbf{r})\right|^2 = 1. \tag{2.6}$$

Introducing now the condensate wave function

$$\psi(\mathbf{r}) = N^{1/2}\psi_s\left(\mathbf{r}\right), \tag{2.7}$$

and the particle density

$$n\left(\mathbf{r}\right) = \left|\psi\left(\mathbf{r}\right)\right|^2, \tag{2.8}$$

the total energy of the system can be written as:

$$H\left(\psi\right) = \int \mathrm{d}^n r \left[\frac{\hbar^2}{2m}|\nabla\psi(\mathbf{r})|^2 + V(\mathbf{r})|\psi(\mathbf{r})|^2 + \frac{g}{2}|\psi(\mathbf{r})|^4\right], \tag{2.9}$$

where $V(\mathbf{r})$ is some external potential. To find the ground state for ψ we can minimize (2.9) with respect to the variations of ψ and ψ^*. This together with the condition that the total number of particles

$$N = \int \mathrm{d}^n r \left|\psi\left(\mathbf{r}\right)\right|^2 \tag{2.10}$$

remains constant can be simultaneously resolved by using Lagrange multipliers. Writing $\delta H - \mu\delta N = 0$, wherein μ is the multiplier that insures the constant total number of atoms constraint. This is equivalent to fixing μ and minimizing $H - \mu N$, that is by doing:

$$\frac{\delta\left(H - \mu N\right)}{\delta\psi^*\left(\mathbf{r}\right)} = 0, \tag{2.11}$$

we obtain

$$-\frac{\hbar^2}{2m}\nabla^2\psi\left(\mathbf{r}\right)+V\left(\mathbf{r}\right)\psi(\mathbf{r})+g|\psi\left(\mathbf{r}\right)|^2\psi\left(\mathbf{r}\right)=\mu\psi\left(\mathbf{r}\right), \tag{2.12}$$

which is the time independent Gross–Pitaevskii Equation (GPE). Similarly, if we minimize the action

$$S=\int_{t_1}^{t_2}L\,\mathrm{d}t\,, \tag{2.13}$$

with the Lagrangian given by

$$L=\int \mathrm{d}^n r\,\frac{i\hbar}{2}\left(\psi^*\frac{\partial\psi}{\partial t}-\psi\frac{\partial\psi^*}{\partial t}\right)-H, \tag{2.14}$$

we obtain

$$i\hbar\frac{\partial\psi(\mathbf{r},t)}{\partial t}=-\frac{\hbar^2}{2m}\nabla^2\psi(\mathbf{r},t)+V(\mathbf{r},t)\psi(\mathbf{r},t)+g|\psi(\mathbf{r},t)|^2\psi(\mathbf{r},t). \tag{2.15}$$

which is the time dependent GPE.

To maintain the consistency between both equations the stationary solutions of Eq. (2.15) must evolve in time as

$$\psi_{stat}(\mathbf{r},t)=e^{-i\mu\frac{t}{\hbar}}\psi_{sol}(\mathbf{r}) \tag{2.16}$$

with ψ_{stat} being a stationary solution of the time dependent GPE (2.15) and ψ_{sol} a solution of the time independent GPE (2.12).

Healing Length

For a free uniform Bose gas with density $n=\frac{N}{Vol}$ and trapping potential $V=0$ Eq. (2.12) becomes

$$g|\psi|^2\psi-\mu\psi=0\rightarrow\mu=g|\psi|^2=gn, \tag{2.17}$$

since $n=|\psi|^2$.

We can then apply a standard nondimensionalization procedure to Eq. (2.12) by doing the following change of variables:

$$\mathbf{r}=\xi\mathbf{r}$$
$$\psi=\sqrt{\frac{\mu}{g}}\psi$$

then

$$-\alpha\nabla^2\psi\left(\mathbf{r}\right)+|\psi\left(\mathbf{r}\right)|^2\psi\left(\mathbf{r}\right)=\psi\left(\mathbf{r}\right)$$

with

$$\alpha = \frac{\hbar^2}{2\xi^2 m\mu}, \tag{2.18}$$

and setting $\alpha = 1$, so that both terms in the left side are of comparable order,

$$\alpha = 1 \rightarrow \xi = \frac{\hbar}{\sqrt{2m\mu}}. \tag{2.19}$$

The quantity ξ is called the healing length and is the length at which the kinetic term, $\nabla^2\psi$, and the interaction term, $g|\psi|^2\psi$ are of comparable order. The healing length gives the minimum distance at which the condensate "heals" back to its bulk density from a localized perturbation and its associated with the size of a quantized vortex core [15, 16].

2.2 Linear Perturbations

We can use Eq. (2.15) to study small perturbations around a uniform condensate.

To achieve that we consider small perturbations in the field ψ, keeping terms up to linear order in the perturbation:

$$\psi(\mathbf{r},t) = \left(\sqrt{n(\mathbf{r})} + \delta\psi(\mathbf{r},t)\right), \tag{2.20}$$

with $\delta\psi(\mathbf{r},t)$ being a small perturbation. Obtaining the pair of equations:

$$i\hbar\frac{\partial\delta\psi(\mathbf{r},t)}{\partial t} = -\frac{\hbar^2}{2m}\nabla^2\delta\psi(\mathbf{r},t) - \mu\delta\psi(\mathbf{r},t) - gn\left(2\delta\psi(\mathbf{r},t) + \delta\psi^*(\mathbf{r},t)\right), \tag{2.21}$$

$$-i\hbar\frac{\partial\delta\psi^*(\mathbf{x},t)}{\partial t} = -\frac{\hbar^2}{2m}\nabla^2\delta\psi^*(\mathbf{r},t) - \mu\delta\psi^*(\mathbf{r},t) - gn\left(2\delta\psi(\mathbf{r},t)^* + \delta\psi(\mathbf{r},t)\right). \tag{2.22}$$

We can diagonalize this system by searching for solutions in the form of

$$\delta\psi(\mathbf{r},t) = e^{i\mu\frac{t}{\hbar}}\left[u(\mathbf{r})e^{-i\omega t} - v^*(\mathbf{r})e^{i\omega t}\right], \tag{2.23}$$

then, inserting (2.23) into (2.21) and (2.22) and isolating the terms of $e^{i\omega t}$ and $e^{-i\omega t}$ leads to the pair of equations

$$\left[-\frac{\hbar^2}{2m}\nabla^2 + 2gn - (\mu + \hbar\omega)\right]u(\mathbf{r}) - gnv(\mathbf{r}) = 0, \tag{2.24}$$

$$\left[-\frac{\hbar^2}{2m}\nabla^2 + 2gn - (\mu - \hbar\omega)\right]v(\mathbf{r}) - gnu(\mathbf{r}) = 0. \tag{2.25}$$

Since we are considering a uniform condensate $\mu = gn$, in momentum space this system becomes algebraic

$$\left[\frac{\hbar^2k^2}{2m} + gn - \hbar\omega\right]u_k - gnv_k = 0, \tag{2.26}$$

$$\left[\frac{\hbar^2k^2}{2m} + gn + \hbar\omega\right]v_k - gnu_k = 0. \tag{2.27}$$

with

$$u(\mathbf{r}) = u_k \frac{e^{i\mathbf{k}\cdot\mathbf{r}}}{\sqrt{V}},$$
$$v(\mathbf{r}) = v_k \frac{e^{i\mathbf{k}\cdot\mathbf{r}}}{\sqrt{V}},$$

where u_k and v_k are amplitudes normalized as $|v_k|^2 - |u_k|^2 = 1$.

Solving the algebraic system leads to:

$$u_k = \frac{\frac{\hbar^2 k^2}{2m} + gn + \hbar\omega}{gn} v_k, \tag{2.28}$$
$$(\hbar\omega)^2 = \frac{\hbar^2 k^2}{2m}\left(\frac{\hbar^2 k^2}{2m} + 2gn\right). \tag{2.29}$$

Equation (2.29) gives the dispersion relationship

$$\hbar\omega = \pm\sqrt{\frac{\hbar^2 k^2}{2m}\left(\frac{\hbar^2 k^2}{2m} + 2gn\right)} \tag{2.30}$$

for small k we have

$$\hbar\omega \sim c\hbar k \tag{2.31}$$

with $c \equiv \sqrt{\frac{gn}{m}}$ being the sound speed.Conselho Nacional de Desenvolvimento Científico e Tecnológico (CNPq) The dispersion relationship, Eq. (2.30), is plotted in Fig. 2.1 where the long and short wavelength behaviours are illustrated.

Figure 2.1: Plot of the dispersion relationship Eq. (2.30) as a function of the wave number expressed in the dimensionless variables $\frac{\hbar\omega}{gn}$ and ξk respectively. The dashed line represents the long wavelength limit and the dotted line the short wavelength limit.

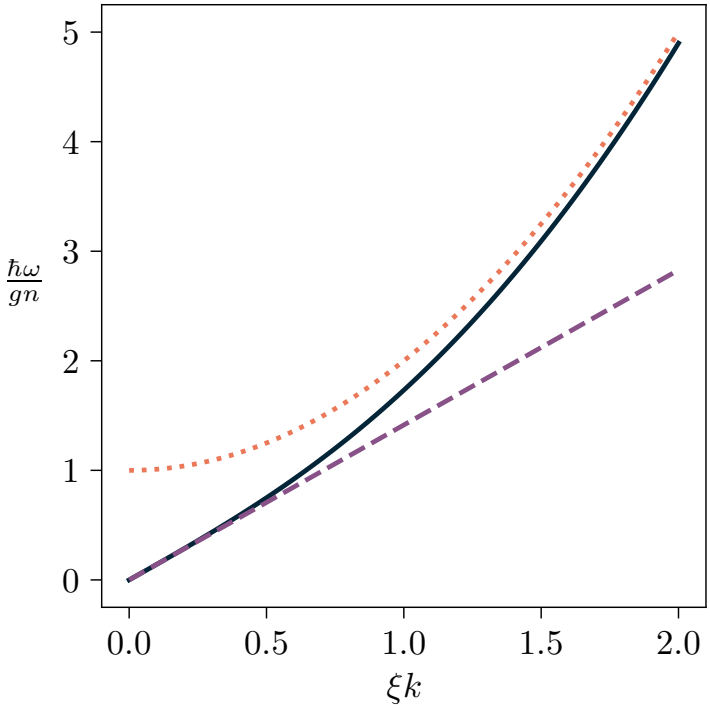

Source: Produced by the author.

The coefficients v_k and u_k can be determined by choosing the energy and imposing the normalization condition, for example considering $\hbar\omega > 0$

$$u_k = \frac{1}{\sqrt{2}}\left(\frac{\Delta_\varepsilon}{\varepsilon_k} + 1\right)^{\frac{1}{2}} \tag{2.32}$$

$$v_k = \frac{1}{\sqrt{2}}\left(\frac{\Delta_\varepsilon}{\varepsilon_k} - 1\right)^{\frac{1}{2}} \tag{2.33}$$

with $\Delta_\varepsilon = \varepsilon_0 + gn$, $\varepsilon_k = \sqrt{\varepsilon_0(\varepsilon_0 + 2gn)}$, $\varepsilon_0 = \xi^2 k^2 gn$ and ξ is the condensate healing length from (2.19).

The full picture of atomic BEC envolves exploring the behaviour of trapped condensates, and the microscopical theory that supports the assumptions of the Gross–Pitaevskii model. Such a discussion goes beyond the intention of this brief overview of the subject but can be found in detail in text books such as [34, 36] and literature reviews [37, 35].

Chapter 3

Turbulence

In the next sections we will briefly review classical and quantum turbulence followed by a slightly more in-depth discussion of wave turbulence.

3.1 Classical Turbulence

State Equations

To describe how a fluid moves we must be able to describe its properties at every point, essentially we need state equations. The most fundamental state equation has to do with the conservation of mass. Since a fluid is a continuous media its velocity is described by a vector field with a velocity vector associated with each point, and its density by a scalar field that describes the distribution of mass in each point. The mass current, or flux, of the fluid is given by

$$\mathbf{j} \equiv \rho \mathbf{v} \tag{3.1}$$

with ρ being the density and $\mathbf{v}$ the velocity field.

The mass conservation equation, called the continuity equation, states that the outward flux of the fluid must be equal to the rate of change of its density, that is:

$$\frac{\partial \rho}{\partial t} + \nabla \cdot (\rho \mathbf{v}) = 0 \tag{3.2}$$

when the density ρ is constant Eq. (3.2) reduces to

$$\nabla \cdot \mathbf{v} = 0 \tag{3.3}$$

and the fluid is said to be incompressible, this is the type of fluid we will concern ourselves hereafter.

The next state equation comes from newton second law of motion. Inside a static fluid the net force per unit volume will be determined by the pressure gradient that balances any external forces, like the effects of gravity. If we generalized gravity to any external force that can be described by a scalar potential then a force balance equation for a static fluid can be stated as

$$-\nabla P - \rho \nabla \Phi = 0 \tag{3.4}$$

with P being the pressure and Φ some external scalar potential.

When we consider a fluid in motion Newton's second law must be accounted for, so the right-hand side in Eq. (3.4) is no longer zero

$$-\nabla P - \rho \nabla \Phi = \rho \mathbf{a} \tag{3.5}$$

the vector a represents the acceleration due to the variation of the velocity field.

It seems intuitive to assume that $\mathbf{a} = \frac{\partial \mathbf{v}}{\partial t}$, but we must be careful, since $\mathbf{v}(\mathbf{r}, t)$ is a vector field, so there will be a difference in the change of velocity between two points in space. We can obtain this difference by writing out the variation in the velocity field due to a variation in time, $t + \Delta t$:

$$\begin{aligned} \Delta \mathbf{v} &= \mathbf{v}(\mathbf{r} + \Delta \mathbf{r}, t + \Delta t) - \mathbf{v}(\mathbf{r}, t) \\ \Delta \mathbf{r} = \mathbf{v} \Delta t \Rightarrow \Delta \mathbf{v} &= \left[(\mathbf{v} \cdot \nabla) \mathbf{v} + \frac{\partial \mathbf{v}}{\partial t} \right] \Delta t \\ \mathbf{a} = \frac{\Delta \mathbf{v}}{\Delta t} &= (\mathbf{v} \cdot \nabla) \mathbf{v} + \frac{\partial \mathbf{v}}{\partial t}. \end{aligned} \tag{3.6}$$

The operator, $\frac{D}{Dt} = \frac{\partial}{\partial t} + \mathbf{v} \cdot \nabla$, is sometimes called the *Lagrangian Derivative* or *Hydrodynamic Derivative*.

Equation (3.5) can now be fully written as

$$\frac{\partial \mathbf{v}}{\partial t} + \mathbf{v} \cdot \nabla \mathbf{v} = -\frac{1}{\rho} \nabla P - \rho \nabla \Phi \tag{3.7}$$

But our balance equation is still not complete, internal forces due the fluid's viscosity and any possible external forces must also be considered therefore the full equation, together with Eq. (3.3), is given by:

$$\begin{aligned} \frac{\partial \mathbf{v}}{\partial t} + \mathbf{v} \cdot \nabla \mathbf{v} &= -\frac{1}{\rho} \nabla P - \rho \nabla \Phi + \nu \nabla^2 \mathbf{v}, \\ \nabla \cdot \mathbf{v} &= 0, \end{aligned} \tag{3.8}$$

with ν being the fluid kinematic viscosity. This pair [1] of equations form the incompressible Navier–Stokes equations, and is the main stage in the exploration of well-developed turbulence.

[1] The incompressible approximation is usually a good approximation for most fluids with a flow speed below that of the sound speed [38, 39].

Turbulence

Turbulence is hard to characterize, usually is easier to look at its features, some of the most important being the chaotic nature and the non-zero vorticity [2] of the system. The Navier–Stokes equations is believed to fully describe the motion of fluids, but it is a very complicated non-linear differential equation and the full set of solutions is not yet generally known.

The main terms that influence the behaviour of the flow in Eq. (3.8) are $\mathbf{v} \cdot \nabla \mathbf{v}$ and $\nu \nabla^2 \mathbf{v}$, the balance between these two terms separates the regimes of well-behaved and smooth flow, called laminar flow, and the chaotic flow dominated by eddies and vortices that is characteristic of turbulent flow.

A quick indicator of these characteristics is the Reynolds number, $Re = \frac{vD}{\nu}$, where D is a characteristic length dependent on the particular system, e.g. the diameter of a pipe, the length of a container, etc. Therefore, a large Reynolds number can serve as a qualitative indicator of the development of turbulence in the system.

In 1928 Richardson proposed [40] that a well-developed turbulent system could be understood in terms of large eddies breaking down into smaller eddies which then in turn further break down in a self-similar process until the smallest eddies would dissipate due to the internal kinematic viscosity of the fluid, this idealized picture is know as the Richardson cascade.

An important quantity to understand the mechanism of the Richardson's cascade is the energy density per unit mass [41, 42] given, in terms of the statistics of the velocity field, by:

$$E = \frac{1}{2}\langle \mathbf{v}(\mathbf{r})\mathbf{v}(\mathbf{r})\rangle = \int_0^\infty \mathcal{E}_k dk \tag{3.9}$$

where $\mathcal{E}_k$ is the energy spectrum. Kolmogorov proposed [43, 25] that for a homogeneous, isotropic and stationary turbulent flow, the energy per unit mass is distributed through a cascade process between the length scales (Fig. 3.1) given by the characteristic length and the length of the smallest eddies before dissipation, also called the Kolmogorov length. Inside this so-called inertial range, the energy spectrum under Kolmogorov's assumptions is determined only by the energy rate and length scale, then the spectrum can be inferred by dimensional analysis:

$$\mathcal{E}_k = K_0 \varepsilon^{\frac{2}{3}} k^{-\frac{5}{3}}. \tag{3.10}$$

where ε is the energy injection rate and K_0 is an experimentally determined constant. This result is known as Kolmogorov-Obukhov Spectrum (K41).

A full discussion of the Kolmogorov-Obukhov theory, its applications and implications can be found in [25, 41, 44].

[2] In the special case of wave turbulence vorticity is replaced by the non-linear interaction between the waves.

Figure 3.1: Illustration of the energy cascade in the inertial range. Large eddies manifest at the energy injection scale and small eddies dissipate near the Kolmogorov length, l_k, scale.

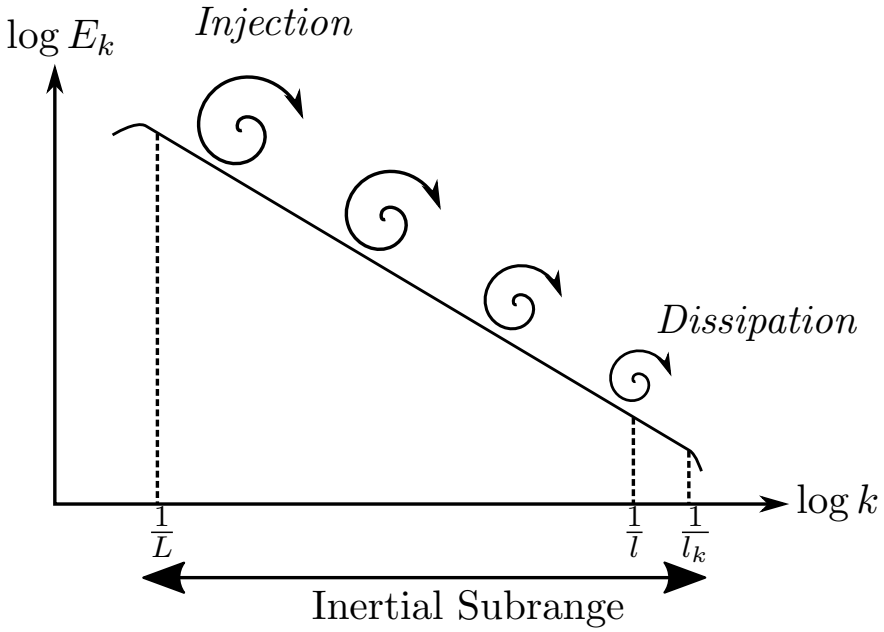

3.2 Quantum Turbulence

The Gross–Pitaevskii model also enable the study of the hydrodynamics of the system. By multiplying the GPE,

$$i\hbar\frac{\partial\psi(\mathbf{r},t)}{\partial t} = -\frac{\hbar^2}{2m}\nabla^2\psi(\mathbf{r},t) + V(\mathbf{r},t)\psi(\mathbf{r},t) + g|\psi(\mathbf{r},t)|^2\psi(\mathbf{r},t), \qquad \text{(2.15 revisited)}$$

by ψ^* and subtracting the complex conjugate we get the continuity equation:

$$\frac{\partial n}{\partial t} + \nabla\cdot(n\mathbf{v}) = 0, \tag{3.11}$$

with velocity field given by:

$$\mathbf{v} = \frac{1}{2i}\frac{(\psi^*\nabla\psi - \psi\nabla\psi^*)}{|\psi|^2}. \tag{3.12}$$

We can further expand this by doing a Madelung transformation,

$$\psi = \sqrt{n}e^{iS},$$

which takes us to two important equations:

$$\mathbf{v} \stackrel{?}{=} \nabla S, \tag{3.13}$$

and

$$\frac{\partial \mathbf{v}}{\partial t} + \nabla\left(\frac{v^2}{2}\right) = -(\frac{1}{\rho}\nabla p + \frac{1}{m}\nabla V) + \frac{1}{m}\nabla\left[\frac{\hbar^2}{2m\sqrt{\rho}}\nabla^2\left(\sqrt{\rho}\right)\right], \tag{3.14}$$

with $\rho = mn$ being the mass density and $p = \frac{n^2 g}{2}$ the pressure.

The symbol $\stackrel{?}{=}$ in Eq (3.13) indicates that the result is wrong and must be corrected. Notice that as a consequence of this result the condensate appears to be irrotational since, $w = \nabla \times \mathbf{v} = \nabla \times \nabla S = 0$. The second equation is an analogue to Eq. (3.8) with zero viscosity, in this case called Euler's equations, the extra term in the right-hand side is called the quantum pressure and is associated with the zero-point motion [34].

Circulation and Vorticity

Equation (3.13) implies that hydrodynamic turbulence is not possible in condensates due to the lack of vorticity, usually this is explained by analysing the circulation of the system.

Since the condensate wave function have to be single-valued and the phase field S is multivalued the change ΔS around a closed contour have to be a multiple of 2π, that is,

$$\Delta S = \oint \nabla S \cdot \mathrm{d}\mathbf{r} = 2\pi\ell, \tag{3.15}$$

with $\ell \in \mathbb{Z}$. The velocity circulation is given by

$$\Gamma = \oint \mathbf{v} \cdot \mathrm{d}\mathbf{r} = \oint \frac{\hbar}{m}\nabla S \cdot \mathrm{d}\mathbf{r} = \frac{\hbar}{m} 2\pi\ell = \ell\frac{h}{m}. \tag{3.16}$$

Equation (3.16) shows that the circulation is quantized in units of h/m. When taking this into consideration a rotating superfluid will have its vorticity equal to zero everywhere except at the location of a vortex line.

An alternative way of dealing with the problem posed by (3.13) is by correcting the hydrodynamic equations by taking into account the multivalued nature of the phase field S [45]. The main idea is that the use of the chain rule in the operation

$$\mathbf{v} = \frac{e^{-iS}\nabla e^{iS} - e^{iS}\nabla e^{-iS}}{2i} \stackrel{?}{=} \nabla S$$

should not be done without care. For example consider a $2D$ isotropic vortex with the phase field defined in the domain $0 \leq S < 2\pi$. Such a vortex can be described in polar coordinates as

$$\psi(\mathbf{r}) = f(\mathbf{r})e^{i\varphi}.$$

Then $S = \varphi$ will be discontinuous at the cut line showed in Fig. 3.2 and

$$\nabla S = \frac{\hat{\varphi}}{r} - 2\pi\Theta(x)\delta(y)\hat{y}. \tag{3.17}$$

A direct calculation of $\mathbf{v}$ will not produce the discontinuities giving simply $\mathbf{v} = \frac{\hat{\varphi}}{r}$.

A correction is then proposed in both the velocity field and the chain rule:

$$\mathbf{v} \to \nabla S + \mathbf{A}, \tag{3.18}$$

$$\nabla e^{iS} \to i\mathbf{v}e^{iS} = i\left(\nabla S + \mathbf{A}\right)e^{iS}, \tag{3.19}$$

where the vector potential $\mathbf{A} = 2\pi\Theta(x)\delta(y)$ compensates for the discontinuities in the phase field S, equation (3.13) is also corrected:

$$w = \nabla \times \mathbf{v} = \nabla \times (\nabla S + \mathbf{A}) = \nabla \times \mathbf{A}, \tag{3.20}$$

which means that the vorticity of the system is contained in the field $\mathbf{A}$.

Figure 3.2: Phase field profile showing a cut line in the positive x axis.

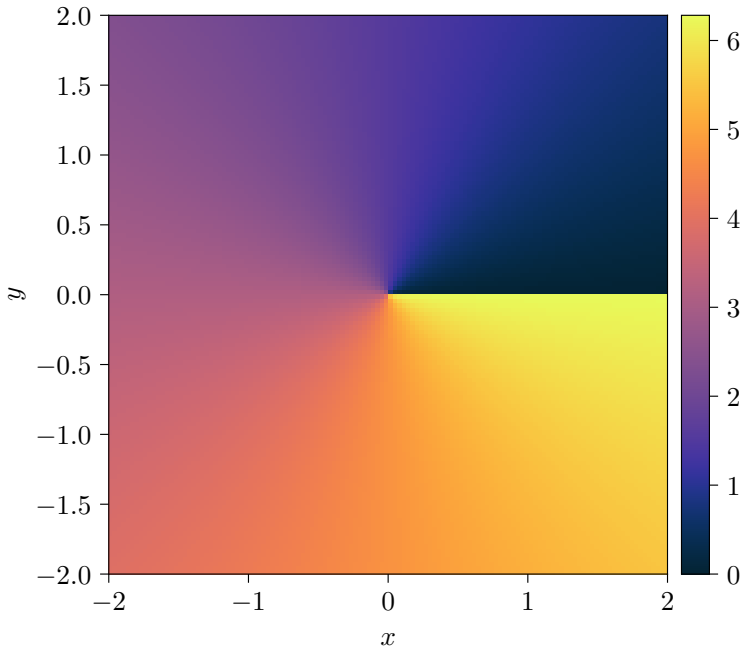

Source: Produced by the author as an adaptation of Ref. [45, Fig. 1].

To account for changes of the type (3.15) the $\mathbf{A}$ field also has to change, otherwise the velocity field would not remain invariant under phase transformations. If we add changes of the type $2\pi\ell$ in the form of a scalar field Q, then we can write the transformation rules as:

$$S \to S + Q, \tag{3.21}$$

$$\mathbf{A} \to \mathbf{A} - \nabla Q, \tag{3.22}$$

being straightforward to check that $\mathbf{v} = \nabla S + \mathbf{A}$ remains invariant under these transformations.

For the arbitrary dimensions case it is convenient to work with Einstein notation where Greek indices are used for both time and space coordinates with values starting from 0, e.g., $\mu = 0, 1, 2, 3$, Latin indices are used for space coordinates with values starting from 1, e.g., $i = 1, 2, 3$ and summation is implied for repeated indices. The velocity field, Eq. (3.12), is then given by

$$v_\mu = \frac{\psi^* \partial_\mu \psi - \psi \partial_\mu \psi^*}{2i} = \frac{e^{-iS}\partial_\mu e^{iS} - e^{iS}\partial_\mu e^{-iS}}{2i} = \partial_\mu S + A_\mu, \tag{3.23}$$

where $\partial_\mu e^{iS} = i(\partial_\mu S + A_\mu)e^{iS}$ is the correction in the chain rule application, the gauge field A_μ is chosen in such away to take into account all possible discontinuities in the phase S so that its derivative does not present any problems. Since the discontinuities can be modified by summing or subtracting a scalar field to S, A_μ has to be modified to take that into account.

The gauge transformations can be generalized as

$$S \to S + Q, \tag{3.24}$$

$$A_\mu \to A_\mu + \partial_\mu Q, \tag{3.25}$$

where Q is a scalar field. For a phase field similar to the $2D$ example used in the beginning $0 \leq S < 2\pi$ the gauge field is $A_\mu = 2\pi\Theta(R)\partial_\mu\Theta(I)$, with R and I being the real and imaginary parts of the wavefunction respectively.

From Eq. (3.23) we can study the velocity flow directly, in order to do that it is convenient to define the force field tensor

$$\begin{aligned} F_{\mu\nu} &= \partial_\mu A_\nu - \partial_\nu A_\mu \\ &= \partial_\mu v_\nu - \partial_\nu v_\mu, \end{aligned} \tag{3.26}$$

then we can write the quantum analog for the Euler equation by writing

$$\partial_0 v_i = F_{0i} + \partial_i v_0. \tag{3.27}$$

Now, from Eq. (3.23), we can write

$$v_0 = \frac{1}{2i}\left(\psi * \partial_0 \psi - \psi \partial_0 \psi^*\right) \tag{3.28}$$

and since

$$\partial_0 \psi = \frac{\partial \psi}{\partial t}, \tag{3.29}$$

we can use Eq. (2.15) to write

$$v_0 = \frac{1}{2}\left(\frac{1}{2\rho}\partial_i\partial_i\rho - \frac{1}{4\rho^2}|\partial_i\rho|^2 - \frac{v_i v_i}{2}\right) - V - g\rho. \tag{3.30}$$

Inserting Eq. (3.30) into Eq. (3.27) we finally obtain

$$\partial_0 v_i = F_{0i} + \partial_i \left[\frac{1}{2} \left(\frac{1}{2\rho} \partial_i \partial_i \rho - \frac{1}{4\rho^2} |\partial_i \rho|^2 - \frac{v_i v_i}{2} \right) - V - g\rho \right]. \tag{3.31}$$

One imediate noticeable difference between Eq. (3.31) and Eq. (3.14) is the added term F_{0i}. As was pointed out in [45] this term corrects the usual equation by providing information about the vorticity of the system. If there are no vorticity in the system then $A_\mu = 0$ and the term F_{0i} vanishes from (3.31). On the other hand, the moment that the vorticity of the system if not zero, the dynamics of the velocity field will be directly affected by the presence of F_{0i}.

Energy Spectrum

A suitable approach to obtain an analogue to the K41 spectrum in quantum turbulence is to write (3.9) in terms of the velocity field (3.12) and directly calculate the spectrum. According to the Helmholtz theorem the velocity field can be separated into its incompressible, $\nabla \cdot \mathbf{v}^\perp = 0$, and compressible, $\nabla \times \mathbf{v}^\parallel = 0$, parts. Then, in analogy with classical turbulence, we can write the incompressible kinetic energy per unit mass as:

$$E = \frac{1}{2} \langle \mathbf{v}^\perp(\mathbf{r}) \mathbf{v}^{\perp *}(\mathbf{r}) \rangle = \int \mathcal{E}_k dk \tag{3.32}$$

where it was assumed that the system is homogeneous and isotropic. We can then obtain the spectrum using the Fourier transform of the velocity field given by:

$$\tilde{\mathbf{v}}^\perp(\mathbf{k}) = \frac{1}{(2\pi)^3} \int \mathbf{v}^\perp(\mathbf{r}) e^{-i\mathbf{k}\cdot\mathbf{r}} dr^3, \tag{3.33}$$

As one can see, due to the nature of the velocity field in Eq. (3.12), this integral can be quite difficult to solve analytically mainly due to the $|\psi|^2$ term in the denominator of $\mathbf{v}$ which would cause discontinuities in any region where the particle density vanishes.

One way of solving this issue is by direct numerical simulation to analyse the energy spectrum [46, 47, 48, 49]. Two regimes [50, 51] were observed, the quasi-classical regime with $\mathcal{E}_k \sim k^{-\frac{5}{3}}$, compatible with Kolmogorv turbulence [52, 53] similar to classical fluids, and the ultraquantum regime [54, 49], with $\mathcal{E}_k \sim k^{-1}$, which was predicted to be compatible with Vinen turbulence. Vinen turbulence differs from Kolmogorv turbulence both in the energy spectrum and the vortex line length decay, and different from classical turbulence is not believed [55, 56] to envolve a self-similar cascade process. The Kolmogorov like turbulence observed in numerical simulations arises in the presence of large vortex tangles and is further characterized by the decay of vortex line length density of order $L \sim t^{-\frac{3}{2}}$ in time, with the vortex dissipation happening at healing length. Vinen turbulence however is dominated by the effects of the immediate neighbourhood of vortices and is characterized by a vortex line density length decay of $L \sim t^{-1}$.

Experimentally proper cascades were observed only in superfluid helium, the closest experimental results for atomic BEC are like the one obtained by Henn et al. [27, 21], but no distinguishable spectrum was observed only the formation of a vortex tangle. A more thorough review of quantum turbulence can be found in Ref. [28, 29, 30].

We intend to present a method for analytically obtain the incompressible energy spectrum directly from the velocity field statistics, for that we will explore the connection between the velocity field and the wavefunction to relate the statistics of the former to the latter.

3.3 Wave Turbulence

Up to this section we discussed turbulence in terms of the non-linear effects of the velocity field, but the GPE (2.15) itself is a non-linear equation. Not only that, but the non-linear term is related to the parameter that controls the interatomic interaction, this makes the atomic BEC a strong candidate for the application of WWT theory.

The WWT theory is an analytical approach developed by Alexander Zakharov [57] as an analogue to the Kolmogorv-Obukhov theory applied to the wave interactions. It consists of a systematic approach to statistically describe the waves of the system and obtain wave spectra analogous to the energy spectra previously mentioned in sections 3.1 and 3.2.

In the following we will describe briefly the main points of the theory and its results, for a more thorough introduction to the subject see [58].

Nondimensionalization

We start by writing Eq. (2.15) in nondimensional units by making the following substitutions

$$\begin{aligned} \mathbf{r} &= \chi \mathbf{r}', \\ t &= \tau t', \\ \psi &= \sqrt{n_0}\psi', \end{aligned}$$

where τ and χ being some characteristic time and distance determined by the boundary conditions of the physical system and $n_0 = \frac{N}{V}$, with N being the total number of particles and V the volume of the system. We will also assume a homogeneous system with trapping potential $V = 0$.

The GPE can then be written as

$$i\frac{\partial \psi'(\mathbf{r}', t')}{\partial t'} = \left[-\alpha\nabla^2 + \beta|\psi'|^2\right]\psi'(\mathbf{r}', t'), \tag{3.34}$$

with

$$\alpha = \frac{\hbar\tau}{2m\chi^2},$$
$$\beta = \frac{gn_0\tau}{\hbar}.$$

We are interested in the case where the effects of the non-linear interaction are weak

$$\alpha = 1 \Rightarrow \tau = \frac{2m\chi^2}{\hbar},$$
$$\therefore \beta = \left(\frac{2gn_0m\chi}{\hbar}\right)^2 = \epsilon^2.$$

Which, dropping the primes, gives the GPE in nondimensional units as

$$i\frac{\partial\psi(\mathbf{r},t)}{\partial t} = -\nabla^2\psi(\mathbf{r},t) + \epsilon^2|\psi|^2\psi(\mathbf{r},t). \tag{3.35}$$

Next we will change to the momentum basis so that the interactions between different wave numbers become explicit.

Fourier Representation

Let us consider that the system is in a periodic box, $\mathbf{r} \in \mathcal{T}$, with period L in all directions, so that:

$$\psi(x + lL, y + mL, z + pL, t) = \psi(x, y, z, t) \tag{3.36}$$

for any $\{l, m, p\} \in \mathbb{Z}$. Then the wavefunction can be represented in Fourier space as

$$\psi(\mathbf{r},t) = \sum_k a(\mathbf{k},t)e^{i\mathbf{k}\cdot\mathbf{r}}, \tag{3.37}$$

$$a(\mathbf{k},t) = \frac{1}{L^D}\int_{\mathcal{T}} \psi(\mathbf{r},t)e^{-i\mathbf{k}\cdot\mathbf{r}}\mathrm{d}^D r. \tag{3.38}$$

with D representing the dimension.

Inserting (3.37) in (3.35) and using (3.38) we end up with

$$i\dot{a}_k - k^2 a_k - \epsilon^2 \sum_{k_1,k_2,k_3} a_{k_1}a_{k_2}a^*_{k_3}\delta_{k_1+k_2,k_3+k} = 0, \tag{3.39}$$

notice that we introduced the following notations:

$$\dot{f} = \frac{df}{dt},$$
$$f(\mathbf{k},t) = f_k,$$
$$\delta_{i,j} = \begin{cases} 1, & i = j \\ 0, & i \neq j \end{cases},$$

with δ representing the Kronecker delta.

As is the case for hydrodynamical turbulence, wave turbulence is not independently sustainable, thus the available wave numbers are finite. Physically these will be determined by the size of the inertial domain, with the smallest and largest available wave numbers being related to the energy injection and energy dissipation scales.

Interaction Picture

Looking at Eq. (3.39) we see that when $\epsilon = 0$ we are left with a simple linear equation

$$i\dot{a}_k - k^2 a_k = 0, \tag{3.40}$$

with general solution $a_k = A_k e^{-i\omega_k t}$, $\omega_k = k^2$ being the dispersion relationship and $A_k \in \mathbb{C}$ a constant complex amplitude. This solution represents the linear limit, where the system is stationary and all the time evolution effects are concentrated in the phase oscillations, with frequency ω_k.

We will now introduce the interaction picture variable,

$$b_k = a_k e^{i\tilde{\omega}_k t}, \tag{3.41}$$

with,

$$\tilde{\omega}_k = \omega_k + \omega_{NL} = \omega_k + 2\epsilon^2 \sum_k |a_k|^2.$$

The ω_{NL} is called the *non-linear frequency shift* and gives the leading contribution to the non-linear effects on the wave dynamics [58]. The effects related to the ω_{NL} cancels out in the interaction picture variable (3.41), this is a result of the interaction parameter of the GPE being independent of the wave number. Now writing Eq. (3.39) in terms of (3.41)

$$i\dot{b}_k = \epsilon^2 \sum_{k_1,k_2\neq k_3} b_{k_1} b_{k_2} b^*_{k_3} e^{i(\omega_{k_3}+\omega_k-\omega_{k_1}-\omega_{k_2})t} \delta_{k_1+k_2,k_3+k}. \tag{3.42}$$

Looking to Eq. (3.42) it seems like we lost some information, since the linear term from Eq. (3.39) apparently vanishes, but no approximations were made, both equations contain the same information. But, the variable b_k essentially separates the time scales of the linear and non-linear regimes, and the time dependence appears in explicit form in the non-linear term on the right-hand side.

Statistical Description

As previously mentioned the WWT theory takes a statistical approach to describe the non-linear wave interactions, therefore we must define which are the statistical variables and assumptions that will be used when applying the theory.

We will assume that the wavefunctions a_k are complex scalar fields and as such can be represented by a phase and an amplitude so that

$$a_l = \sqrt{J_l}\Phi_l, \tag{3.43}$$

whit $J_l \in \mathbb{R}^+$ being the amplitude of the mode l and $\Phi_l \in \mathbb{S}^1$ its phase factor. Note that $\mathbb{S}^1$ represents the unitary circle, i.e., $\Phi_l = e^{i\varphi_l}$ and $\varphi_l \in [0, 2\pi)$.

For the statistical quantities we will consider the following definitions [58]:

Definition 1 (Random Phase and Amplitude (RPA))**.** A complex field a_l is said to be of RPA type if the following is true:

- Both the phase and amplitude of a_l are independent random variables.
- The phase has a uniform distribution over $\mathbb{S}^1$.

Definition 2 (Moment-Generating Function)**.** The moment-generating function for each mode l is given by:

$$\mathscr{L}_l\{\lambda_l\} = \left\langle \exp\left[\left(\frac{L}{2\pi}\right)^D J_l\lambda_l\right]\right\rangle, \tag{3.44}$$

with $\lambda_l \in \mathbb{R}$ and $\langle\cdots\rangle$ representing the average.

Definition 3 (Probability Density Function)**.** The probability density function for each mode l is given by the inverse Laplace transform of (3.44):

$$\mathscr{P}_l = \frac{1}{2i\pi}\int_{\zeta-i\infty}^{\zeta+i\infty} e^{-\lambda_l}\mathscr{L}_l\{\lambda_l\}\,\mathrm{d}\lambda_l\,, \tag{3.45}$$

where ζ must be chosen in such a way that the integration contour is to the right of all singularities of $\mathscr{L}_l\{\lambda_l\}$ in the complex λ_l-plane.

Definition 4 (Wave Spectrum)**.** The wave spectrum is defined as:

$$n_l = \left(\frac{L}{2\pi}\right)^D \langle J_l\rangle\,, \tag{3.46}$$

or in terms of the probability density function

$$\begin{aligned} n_l &= [\partial_{\lambda_l}\left\langle e^{\lambda_l(\frac{L}{2\pi})^D J_l}\right\rangle]_{\lambda_l=0} = [\partial_{\lambda_l}\mathscr{L}\lambda_l]_{\lambda_l=0} \\ &= \left(\frac{L}{2\pi}\right)^D \int_0^\infty s_l\mathscr{P}(s_l)\,\mathrm{d}s_l\,. \end{aligned} \tag{3.47}$$

Theorem 1 (Wick Contraction Rule)**.** *For a field of type RPA averages of multiple fields can be reduced by applying the following rule of thumb: If the number of conjugated fields "a^*" is different to the number of non-conjugated fields"a" then the average is 0. In the case they are equal then the average is the sum of all possible pairwise combinations of conjugated and non-conjugated terms*[3]*, for instance:*

$$\begin{aligned}
\left\langle a_{l_1} a_{l_2} a^*_{l_3} a^*_{l_4} \right\rangle &= \left\langle J_{l_1} J_{l_2} \right\rangle_J \left\langle \Phi_{l_1} \Phi_{l_2} \Phi^*_{l_3} \Phi^*_{l_4} \right\rangle_\Phi \\
&= \left\langle J_{l_1} J_{l_2} \right\rangle_J \left(\delta_{l_1,l_3}\delta_{l_2,l_4} + \delta_{l_1,l_4}\delta_{l_2,l_3} - \delta_{l_1,l_2}\delta_{l_1,l_3}\delta_{l_1,l_4}\right) \\
\left\langle J_{l_1} J_{l_2} \right\rangle_J &= \begin{cases} \left\langle J_{l_1} \right\rangle \left\langle J_{l_2} \right\rangle & l_1 \neq l_2 \\ \left\langle J^2_{l_1} \right\rangle & l_1 = l_2 \end{cases} \\
\Rightarrow \left\langle a_{l_1} a_{l_2} a^*_{l_3} a^*_{l_4} \right\rangle &= \left\langle J_{l_1} \right\rangle \left\langle J_{l_2} \right\rangle \left(\delta_{l_1,l_3}\delta_{l_2,l_4} + \delta_{l_1,l_4}\delta_{l_2,l_3}\right) + \left(\left\langle J^2_{l_1} \right\rangle - 2\left\langle J_{l_1} \right\rangle^2\right)\delta_{l_1,l_2}\delta_{l_1,l_3}\delta_{l_1,l_4}.
\end{aligned} \tag{3.48}$$

Power Series Expansion

To construct our solution we will consider a period τ that is larger than the linear period $\tau_L \sim \frac{2\pi}{\omega_k}$, but not so large that the system is dominated by the non-linear dynamics. From Eq. (3.42) we see that the time evolution of b_k is of order ϵ^2 for the first order time derivative, with that in mind a convenient intermediary time scale is $\tau \sim \frac{2\pi}{\epsilon^2\omega_k}$ so

$$\frac{2\pi}{\omega_k} \ll \tau \ll \frac{2\pi}{\epsilon^4\omega_k},$$

then we can expand b_k in the instant $t = \tau$ in powers of ϵ,

$$b_k(\tau) = \sum_{j=0}^{\infty} \epsilon^{2j} b_k^{(j)}(\tau). \tag{3.49}$$

To use (3.49) as a solution we need at least an initial state, so that the full series can be built upon the $0th$ order term. Notice that at order ϵ^0 we must have $b_k^{(0)}$ independent of τ, so it makes sense to take $b_k^{(0)} = b_k(0)$.

We can now calculate each term iteratively by using each preceding order to obtain the next, as such the $b_k^{(1)}$ is given by solving

$$i\dot{b}_k^{(1)} = \sum_{k_1,k_2\neq k_3} b_{k_1}^{(0)} b_{k_2}^{(0)} b_{k_3}^{(0)^*} e^{i(\omega_{k_3}+\omega_k-\omega_{k_1}-\omega_{k_2})t}\delta_{k_1+k_2,k_3+k} \tag{3.50}$$

which gives

$$b_k^{(1)}(\tau) = -i \sum_{k_1,k_2\neq k_3} b_{k_1}(0) b_{k_2}(0) b^*_{k_3}(0) \Delta_\tau(\Omega(k,k_3,k_1,k_2))\delta_{k_1+k_2,k_3+k}, \tag{3.51}$$

[3]The proof follows from Def. 1 and Def. 3 [58, see Sec. 5.6].

with

$$\Omega(l,k,m,n) = \omega_l + \omega_k - \omega_m - \omega_n,$$

and

$$\Delta_\tau(x) = \int_0^\tau e^{ixt}\,\mathrm{d}t\,.$$

For the $b_k^{(2)}$ term we must solve

$$\begin{aligned} i\dot{b}_k^{(2)} = &\sum_{k_1,k_2\neq k_3} b_{k_1}^{(0)} b_{k_2}^{(0)} b_{k_3}^{(1)^*} e^{i(\omega_{k_3}+\omega_k-\omega_{k_1}-\omega_{k_2})t}\delta_{k_1+k_2,k_3+k} \\ &+ 2\sum_{k_1,k_2\neq k_3} b_{k_1}^{(1)} b_{k_2}^{(0)} b_{k_3}^{(0)^*} e^{i(\omega_{k_3}+\omega_k-\omega_{k_1}-\omega_{k_2})t}\delta_{k_1+k_2,k_3+k}, \end{aligned} \tag{3.52}$$

the 2 in the second term on the right-hand side comes from the symmetry created by exchanging $k_1 \leftrightarrow k_2$ indices in the summation.

Using the zeroth and first orders and integrating we end up with

$$b_k^{(2)}(\tau) = P_k + 2Q_k \tag{3.53}$$

with

$$\begin{aligned} P_k = \sum_{k_1,k_2\neq k_3,k_4,k_5\neq k_6} &\big[b_{k_1}(0)b_{k_2}(0)b_{k_4}^*(0)b_{k_5}^*(0)b_{k_6}(0) \\ &\times E_\tau(\Omega(k,k_3,k_1,k_2),\Omega(k_4,k_5,k_3,k_6))\delta_{k_1+k_2,k_3+k}\delta_{k_4+k_5,k_6+k_3}\big]\,, \end{aligned} \tag{3.54}$$

and

$$\begin{aligned} Q_k = \sum_{k_2\neq k_3,k_4,k_5\neq k_6} &\big[b_{k_4}(0)b_{k_5}(0)b_{k_6}^*(0)b_{k_2}(0)b_{k_3}^*(0) \\ &\times E_\tau(\Omega(k,k_3,k_1,k_2),\Omega(k_1,k_6,k_4,k_5))\delta_{k_1+k_2,k_3+k}\delta_{k_4+k_5,k_6+k_1}\big]\,, \end{aligned} \tag{3.55}$$

where

$$E_\tau(x,y) = \int_0^\tau e^{i(x-y)t}\,\mathrm{d}t\,.$$

Higher order terms can be obtained similarly.

Moment Generating Function

The next step is calculate the statistical quantities. Once we have the moment generating function 2 we can obtain all the other relevant quantities. The moment generating function at instant τ can be obtained by taking

$$J_k(\tau) = |b_k(\tau)|^2 \tag{3.56}$$

and using Eq. (3.44) leading to

$$\mathscr{L}_k(\tau) = \left\langle \exp\Big(|b_k(\tau)|^2 \, \tilde{\lambda}_k \Big) \right\rangle$$

with $\tilde{\lambda}_k = \left(\frac{L}{2\pi}\right)^D \lambda_k$ for convenience. Resulting in

$$\begin{aligned}\mathscr{L}_k(\tau) &\approx \left\langle \exp\left\{ \tilde{\lambda}_k \left| b_k^{(0)} + \epsilon^2 b_k^{(1)} + \epsilon^4 b_k^{(2)} \right|^2 \right\} \right\rangle \\ &= \left\langle \exp\left\{ \tilde{\lambda}_k \left[\left| b_k^{(0)} \right|^2 + \epsilon^2 \left(b_k^{(0)*} b_k^{(1)} + \text{c.c} \right) + \epsilon^4 \left(\left| b_k^{(1)} \right|^2 + b_k^{(0)*} b_k^{(2)} + \text{c.c} \right) \right] \right\} \right\rangle,\end{aligned}$$

where we only kept terms up to the order of ϵ^4 in $b_k(\tau)$ and $c.c$ represents the complex conjugate. The exponential in the right-hand side can be also be expanded in power of ϵ

$$\begin{aligned}\mathscr{L}_k(\tau) &= \left\langle e^{\tilde{\lambda}_k J_k^{(0)}} \exp\left\{ \tilde{\lambda}_k \left[\epsilon^2 (b_k^{(0)*} b_k^{(1)} + \text{c.c}) + \epsilon^4 (|b_k^{(1)}|^2 + b_k^{(0)*} b_k^{(2)} + \text{c.c}) \right] \right\} \right\rangle \\ &\approx \left\langle e^{\tilde{\lambda}_k J_k^{(0)}} (1 + \epsilon^2 \alpha 1_k + \epsilon^4 \alpha 2_k) \right\rangle,\end{aligned} \tag{3.57}$$

with

$$\alpha 1_k = \tilde{\lambda}_k (b_k^{(0)*} b_k^{(1)} + c.c), \tag{3.58}$$

$$\alpha 2_k = \tilde{\lambda}_k [(|b_k^{(1)}|^2 + b_k^{(0)*} b_k^{(2)} + \text{c.c}) + \frac{\tilde{\lambda}_k}{2} (2|b_k^{(0)}|^2 |b_k^{(1)}|^2 + (b_k^{(0)*} b_k^{(1)})^2 + \text{c.c})]. \tag{3.59}$$

We need to solve the averages in (3.57), for that we will consider that at $t = 0$ we have $b_k(0) = a_k(0)$. Taking $a_k(0)$ as a RPA field, as defined in **Definition** 1, the averages can be reduced using the Wick contraction rule and in combination with the following relationships

$$\begin{aligned}\langle J_l \rangle &= \left(\frac{2\pi}{L}\right)^D n_l, \\ \left\langle e^{\lambda_k J_l} \right\rangle &= \mathscr{L}_l, \\ \left\langle J_l e^{\lambda_l J_l} \right\rangle &= \left(\frac{L}{2\pi}\right)^D \frac{\partial \mathscr{L}_l}{\partial \lambda_l},\end{aligned}$$

we can obtain the expression:

$$\begin{aligned}&\mathscr{L}_k(\tau) - \mathscr{L}_k(0) = \\ &2\epsilon^4 \left(\frac{2\pi}{L}\right)^{2D} \left[\left(\lambda_k \mathscr{L}_k + \lambda_k^2 \frac{\partial \mathscr{L}_k}{\partial \lambda_k} \right) \sum_{k_1,k_2,k_3} n_{k_1} n_{k_2} n_{k_3} \delta_{k+k_3,k_1+k_2} |\Delta_\tau(\Omega(k,k_3,k_1,k_2))|^2 \right. \\ &\left. + 2\lambda_k \frac{\partial \mathscr{L}_k}{\partial \lambda_k} \sum_{k_1,k_2,k_3} [n_{k_1} n_{k_2} - n_{k_3}(n_{k_1} + n_{k_2})] \delta_{k+k_3,k_1+k_2} \mathcal{R}(E(-\Omega(k,k_3,k_1,k_2), \Omega(k,k_3,k_1,k_2))) \right].\end{aligned} \tag{3.60}$$

We follow by taking the large box limit and the weak non-linearity limit, $L \to \infty$ and $\epsilon \to 0$. The large box limit leads to the following rules of thumb:

$$\sum_{k_1,k_2,k_3} \Rightarrow \left(\frac{L}{2\pi}\right)^{3D} \int \mathrm{d}^D k_1 \, \mathrm{d}^D k_2 \, \mathrm{d}^D k_3 \,, \tag{3.61}$$

$$\text{Kronecker–}\delta \Rightarrow \left(\frac{2\pi}{L}\right)^{D} \text{Dirac–}\delta. \tag{3.62}$$

For the weak non-linearity limit we remember that we set

$$\frac{2\pi}{\omega_k} \ll \tau \ll \frac{2\pi}{\epsilon^4 \omega_k},$$

with $\tau \sim \frac{2\pi}{\epsilon^2 \omega_k}$, so $\tau \to \infty$ as $\epsilon \to 0$, which leads to the approximation

$$\frac{\mathscr{L}_k(\tau) - \mathscr{L}_k(0)}{\tau} \approx \dot{\mathscr{L}}_k. \tag{3.63}$$

and the following limits

$$\lim_{\tau\to\infty} |\Delta_\tau(x)|^2 = 2\pi\tau\delta(x), \tag{3.64}$$

$$\lim_{\tau\to\infty} \mathcal{R}(E(-x,x)) = \pi\tau\delta(x), \tag{3.65}$$

with $x = \omega_k + \omega_{k_3} - \omega_{k_1} - \omega_{k_2}$, the emergence of the characteristic Dirac delta behaviour can be observed in Fig. 3.3. Notice that this process is similar to the continuous limit in the transition between two energy eigenstates given by Fermi's golden rule of quantum mechanics, the difference here being that in the quantum mechanics case there are only two frequencies involved, the frequency of te initial state and the frequency of the final state after the perturbation, while is this case we have four frequencies due to the non-linear interaction between the waves.

Equation (3.60) becomes the time evolution equation of the moment-generating function

$$\dot{\mathscr{L}}_k = \lambda_k \eta_k \mathscr{L}_k + (\lambda_k^2 \eta_k - \lambda_k \gamma_k) \frac{\partial \mathscr{L}_k}{\partial \lambda_k}, \tag{3.66}$$

with

$$\eta_k = 4\pi\epsilon^4 \int \delta(\mathbf{k} + \mathbf{k}_3 - \mathbf{k}_1 - \mathbf{k}_2)\delta(\Omega(k, k_3, k_1, k_2)) n_{k_1} n_{k_2} n_{k_3} \, \mathrm{d}^D k_1 \, \mathrm{d}^D k_2 \, \mathrm{d}^D k_3 \,, \tag{3.67}$$

$$\gamma_k = 4\pi\epsilon^4 \int \delta(\mathbf{k} + \mathbf{k}_3 - \mathbf{k}_1 - \mathbf{k}_2)\delta(\Omega(k, k_3, k_1, k_2))[n_{k_3}(n_{k_1} + n_{k_2}) - n_{k_1} n_{k_2}] \, \mathrm{d}^D k_1 \, \mathrm{d}^D k_2 \, \mathrm{d}^D k_3 \,. \tag{3.68}$$

Kinetic Equation

We can obtain the evolution equation for the probability density function by using the inverse Laplace transform on Eq. (3.66)

$$\dot{\mathscr{P}}_k = \frac{\partial}{\partial s_k}\left(s_k(\gamma_k \mathscr{P}_k + \eta_k \frac{\partial \mathscr{P}_k}{\partial s_k}) \right). \tag{3.69}$$

Figure 3.3: Behaviour of $|\Delta_T|^2$ for increasing period T.

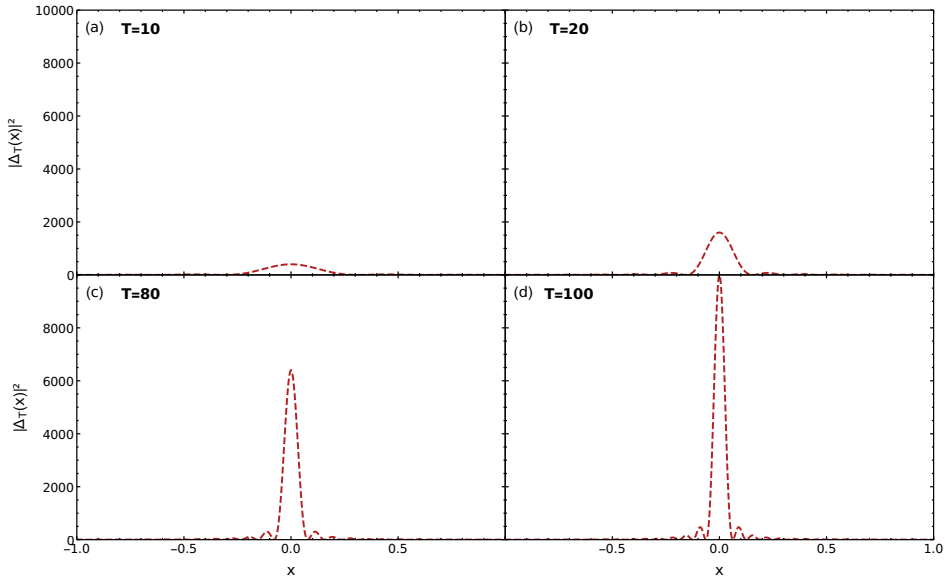

Source: Produced by the author.

Notice that Eq. (3.69) is a continuity equation and the right-hand side can be interpreted as a probability flux, this guarantees probability conservation.

Then using the Definition 4 of the wave spectrum

$$n_k = \int_0^\infty s_k \mathscr{P}_k \, \mathrm{d}s_k \,,$$

and using Eq. (3.69)

$$\dot{n}_k = -\int_0^\infty (s_k \gamma_k \mathscr{P}_k + s_k \eta_k \frac{\partial}{\partial s_k} \mathscr{P}_k) \, \mathrm{d}s_k \,, \tag{3.70}$$

Integrating the right-hand side by making use of integral by parts and the unitary nature of the probability density function, leading to

$$\dot{n}_k = \eta_k - \gamma_k n_k. \tag{3.71}$$

Then inserting Eq. (3.67), Eq. (3.68) and $\Omega(l,k,m,n) = \omega_l + \omega_k - \omega_m - \omega_n$ into Eq. (3.71), we obtain the kinetic equation

$$\begin{aligned} \dot{n}_k = 4\pi\epsilon^4 \int n_k n_{k_1} n_{k_2} n_{k_3} \left[\frac{1}{n_k} + \frac{1}{n_{k_3}} - \frac{1}{n_{k_1}} - \frac{1}{n_{k_2}}\right] \\ \times \delta(\mathbf{k} + \mathbf{k}_3 - \mathbf{k}_1 - \mathbf{k}_2)\delta(k^2 + k_3^2 - k_1^2 - k_2^2) \, \mathrm{d}^D k_1 \, \mathrm{d}^D k_2 \, \mathrm{d}^D k_3 \,. \end{aligned} \tag{3.72}$$

Equation (3.72) describes the evolution of the wave number distribution, n_k. The delta functions in the right-hand side integral guarantees conservation of momentum and of kinetic energy and also characterize the system.

3.4 Wave Spectrum Cascades

In general, we can write for a conserved quantity Φ with associated density ρ_k:

$$\Phi = \int \rho_k n_k \, \mathrm{d}^D k = \text{const.} \tag{3.73}$$

For our system we have two conserved quantities, the total energy E with energy density $\mathcal{E}_k = \omega_k n_k$ and the total number of particles N with density $\rho_k = 1$.

$$E = \int \mathrm{d}^D k \, \omega_k n_k = \text{const}, \tag{3.74}$$

$$N = \int \mathrm{d}^D k \, n_k = \text{const.} \tag{3.75}$$

For each statistical invariant a stationary solution to the kinetic equation can be constructed by looking for solutions of n_k that maintain a constant flux. Zakharov [57] developed a systematic approach to obtain these solutions that makes use of isotropic and homogeneity assumptions. For 4-wave systems with a general interaction parameter $W(\mathbf{k}, \mathbf{k}_1, \mathbf{k}_2, \mathbf{k}_3)$ the homogeneity considerations are stated as

$$\left.\begin{aligned} \omega(\lambda k) &= \lambda^\alpha \omega(k) \\ W(\lambda\mathbf{k}, \lambda\mathbf{k}_1, \lambda\mathbf{k}_2, \lambda\mathbf{k}_3) &= \lambda^\beta W(\mathbf{k}, \mathbf{k}_1, \mathbf{k}_2, \mathbf{k}_3) \\ n(k) &\sim k^\nu \end{aligned}\right\} \Longrightarrow \begin{aligned} n_{\mathcal{N}}(k) &\sim k^{-D-2\beta/3+\alpha/3} \\ n_{\mathcal{E}}(k) &\sim k^{-D-2\beta/3} \end{aligned} \tag{3.76}$$

with $n_{\mathcal{N}}$ being the solution associated with conservation of number of particles and $n_{\mathcal{E}}$ the solution associated with energy conservation. For our system we have specifically:

$$\left.\begin{aligned} \omega(k) &= k^2 \\ W^{kk_1}_{k_2k_3} &= g \sim k^0 \end{aligned}\right\} \Longrightarrow \begin{aligned} n_{\mathcal{N}}(k) &= k^{-D+2/3} \\ n_{\mathcal{E}}(k) &= k^{-D} \end{aligned} \tag{3.77}$$

Due to its similarities with the velocity field related spectrum of hydrodynamic turbulence these solutions are called Kolmogorov-Zakharov spectra. This state was experimentally verified, both with harmonic [59] and box like [60, 61] traps.

There has been great effort exploring these solutions, the most complete numeric simulation of the $3D$ case was done by Proment, Nazarenko, and Onorato [62, 63]. By introducing a forcing term for large k in combination with a dissipative term for small k they managed to observe stationary behaviour and measure both spectra in agreement with the theoretical predictions.

It was also observed that without the dissipation at small k there is rapidly accumulation of particles in the ground state leading to a breakdown of the 4-wave turbulence. The system then undergoes a transition to a 3-wave turbulence system that can be understood by redeveloping the theory but starting from Eq. (2.21) and Eq. (2.22) instead. This system can also be studied numerically, see for example [64].

In the transition between the 4-wave and 3-wave systems a different type of spectrum was observed [62] that could not be immediately understood from the WWT predictions. It was called the "critical balance" spectrum [58, Chap 15] and argued to be a consequence of the kinetic energy and interaction energy being of comparable order, resulting in a spectrum of type $n(k) \sim k^{-4}$.

In summary the WWT is a well tested and fully developed theoretical tool to describe wave interactions in a weakly interacting regime. In the next chapter we will propose a method to connect the statistics of the velocity field with the statistics of the wavefunction enabling us to analytically calculate the incompressible energy spectrum.

Chapter 4

Energy Spectra in the WWT Regime

In Chapter 2 we showed that an atomic BEC can be described by the Gross–Pitaevskii Equation (GPE) (2.15). In Section 3.2 we showed the hydrodynamic equations and how a correction is needed to account for the multivalued nature of the condensate phase and recover from the apparent irrotational nature of the condensate. Lastly in section 3.3 we explored the WWT theory and how the non-linearity of the GPE leads to an analogue to the K41 in the condensate wave distribution.

In the following we will combine the hydrodynamics of the Gross–Pitaevskii model with the wave statistics of the WWT theory to analytically obtain the incompressible energy spectrum directly from the velocity field statistics.

4.1 Auxiliary Wavefunction

One of the main problems in an analytical calculation of the incompressible energy spectrum is in how to account for the discontinuities in the velocity field caused by the vortices. To deal with this obstacle we remember that the incompressible energy spectrum depends only on the incompressible part of the velocity field. In Section 3.2 we discussed how the corrected velocity field is represented [see 45]

$$\mathbf{v} = \nabla S + \mathbf{A} \tag{4.1}$$

with S being the phase and $\mathbf{A}$ the vector potential where all discontinuities are concentrated.

Keeping our convention of $0 \leq S < 2\pi$ for the phase we construct an auxiliary wavefunction (4.2) for which the vector potential $\mathbf{A} = 2\pi\Theta(R)\boldsymbol{\nabla}\Theta(I)$ appears directly on the particle current, in this way no discontinuities need to be dealt with.

$$\phi \equiv \frac{\sqrt{\pi}}{2}\left(\text{sign}(R) + i\ \text{sign}(I)\right) \tag{4.2}$$

with $R = \mathrm{Re}\,\psi$ and $I = \mathrm{Im}\,\psi$.

Before we proceed to analytically calculate the energy spectrum we need to verify the auxiliary wavefunction statistical properties. We must specially make sure if any of the WWT theory results are still valid.

One way of investigating the validity of the auxiliary wavefunction (4.2) is numerically. Since the waveturbulence state is already validated in the literature no direct simulation of the GPE is needed, instead we construct the wavefunction in the WWT state and calculate the resulting wavefunction ϕ. Then we verify by direct calculation if the RPA state and closure condition are preserved.

Numerical Verification

First let us consider our system to be in the wave turbulent regime so that $\tilde{\psi}(\mathbf{k}) \sim |\mathbf{k}|^{\frac{\alpha}{2}} e^{iS}$, with $\alpha \in \mathbb{R}$ being the power-law coefficient of a stationary $n(k) \sim k^{\alpha}$ and $0 \leq S < 2\pi$ a random phase uniformly distributed in this interval.

Numerically, we initialize $\tilde{\psi}(k)$ in a 1024^3 grid in Fourier space, and generate the phase field S as a uniform distribution in the $0 \leq S < 2\pi$ interval for each point $\mathbf{k}$ in the grid. We then numerically obtain $\psi(r)$ by using the inverse Fourier transform and construct the auxiliary wavefunction $\phi(r)$ as described by Eq. (4.2). We proceed by applying the direct Fourier transform to obtain $\tilde{\phi}(k)$.

By averaging the field over multiple samples we verify that S remains uniformly random in momentum space, and observe that the density in real space is homogeneous for the auxiliary wavefunction as can be seen in Fig. 4.1.

In addition to the randomness preservation we also see that the closure condition of the two-point correlation is preserved as can be seen from, Fig. 4.2 which shows that ϕ has no correlation between different wave numbers, this was done by directly calculating $\langle \tilde{\phi}(\mathbf{k}) \tilde{\phi}^*(\mathbf{k}') \rangle$, over multiple samples and averaging the results.

We also observed that $\tilde{\phi}(k)$ will have a power-law wave spectrum, k^{β}, preserving both the statistical properties and the nature of the stationary solutions of the kinetic equation. To obtain the relationship between the coefficients β and α we prepared several configurations of $\tilde{\psi}(k)$ with different coefficients α, and calculated the induced power-law coefficient β for the auxiliary wavefunction, the results can be seen on Fig. 4.3. Surprisingly we found that $\beta = \alpha$, in the domain of coefficients predicted by WWT, $-3 \geq \alpha \leq -\frac{7}{3}$, as shown by the best fit coefficients, the special case of $\alpha = -3$ is shown as an example in Fig. 4.4. Therefore, in the following we will consider $n_{\psi}(k) \sim n_{\phi}(k)$.

With that we numerically demonstrated that inside the limits of the WWT the auxiliary wavefunction $\tilde{\phi}(k)$ has similar statistical properties to the system's wavefunction $\tilde{\psi}(k)$. Par-

Figure 4.1: Density and phase profiles of the original wavefunction, ψ and auxiliary wavefunction ϕ. We see that while the density of the auxiliary wavefunction is homogeneous the randomness of the phase field in phase space appears to be preserved.

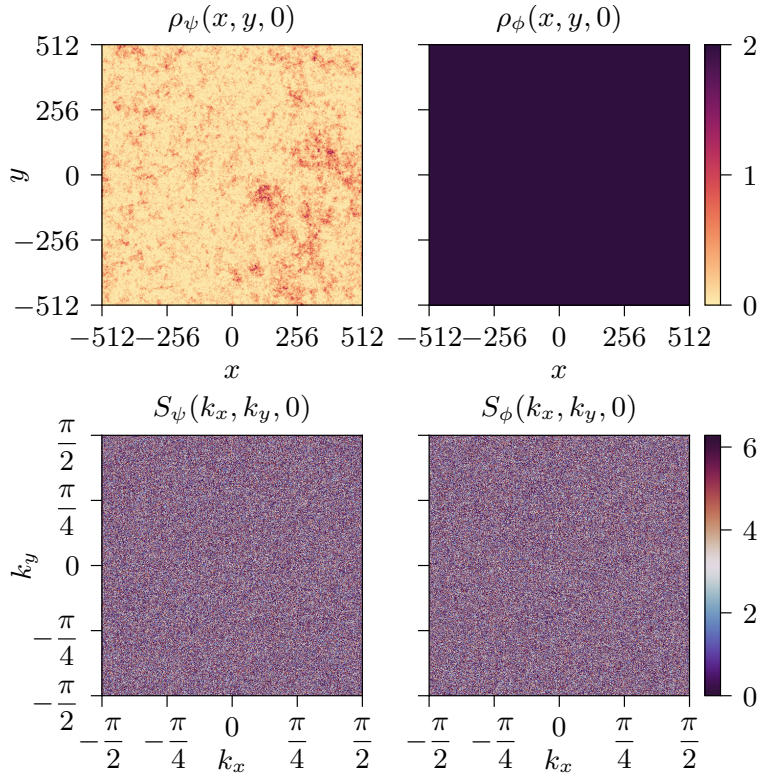

Source: Produced by the author.

ticularly, the wave spectrum of both fields obey the same power-law, this will enable us to analytically calculate the incompressible energy spectrum of the system.

4.2 Incompressible Velocity Field

A direct calculation of the velocity field, shows that $\mathbf{v}_\phi = \frac{2}{\pi}\mathbf{j}_\phi$, with:

$$\mathbf{j}_\phi = \frac{\phi^*\nabla\phi - \phi\nabla\phi^*}{2i} = \frac{\pi}{2}\left(\text{sign}(R) + 1\right)\nabla\text{sign}(I) - \frac{\pi}{4}\nabla[(\text{sign}(R) - 2)\text{sign}(I)] \tag{4.3}$$

where the subscript ϕ indicates that the quantity is calculated in relation to the auxiliary wavefunction ϕ, showing that the velocity and current fields are proportional to each other.

Now, taking $\frac{\pi}{2}\left(\text{sign}(R) + 1\right)\nabla\text{sign}(I)$, from the right-hand side of (4.3) and making the following substitution:

$$\text{sign}(a) = 2\Theta(a) - 1,$$
$$\Rightarrow \frac{\pi}{2}\left(\text{sign}(R) + 1\right)\nabla\text{sign}(I) = 2\pi\Theta(R)\nabla(\Theta(I)) = \mathbf{A},$$

Figure 4.2: Cross-section of the 2 point correlator of the auxiliary wavefunction ϕ. Note that the correlation is zero everywhere except when $\mathbf{k} = \mathbf{k}'$ demonstrating the closure condition of the wave spectrum, i.e., $\langle\tilde{\phi}(\mathbf{k})\tilde{\phi}^*(\mathbf{k}')\rangle = \langle|\tilde{\phi}(\mathbf{k})|^2\rangle\delta(\mathbf{k}-\mathbf{k}')$.

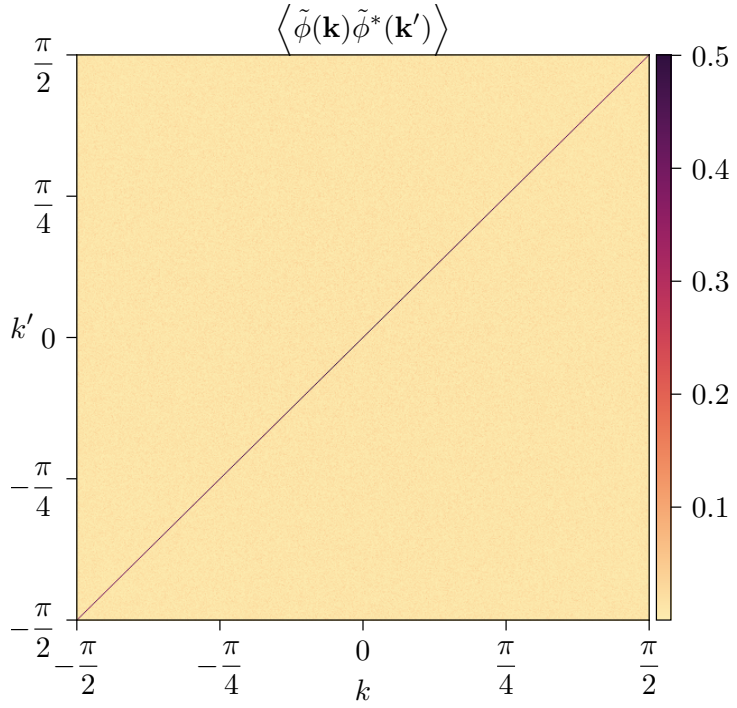

Source: Produced by the author.

then:

$$\mathbf{j}_\phi = \mathbf{A} - \frac{\pi}{4}\nabla[(\text{sign}(R)+2)\text{sign}(I)] \tag{4.4}$$

where $\mathbf{A}$ is the vector that carries the information about the incompressible part of the system. This result shows that $\mathbf{v}^\perp = \frac{\pi}{2}\mathbf{v}_\phi^\perp$, that is, the incompressible part of the velocity field of the wavefunction ψ is proportional to that of the auxiliary wavefunction ϕ.

4.3 Incompressible Energy Spectrum

Now we will show that one can infer the statistics of the incompressible velocity field directly from the statistics of the wavefunction itself as long as the system is in a regime where the full statistical description of the waves are known, such is the case of the weak wave turbulent regime.

Figure 4.3: Comparison between power-law coefficients of $n_\psi(k)$ and $n_\phi(k)$, the horizontal axis represents the prepared coefficients for the ψ wavefunction and the vertical axis the β coefficient obtained from the calculated wave spectrum of the ϕ wavefunction. The straight line shows the best fit approximation using a standard linear regression algorithm.

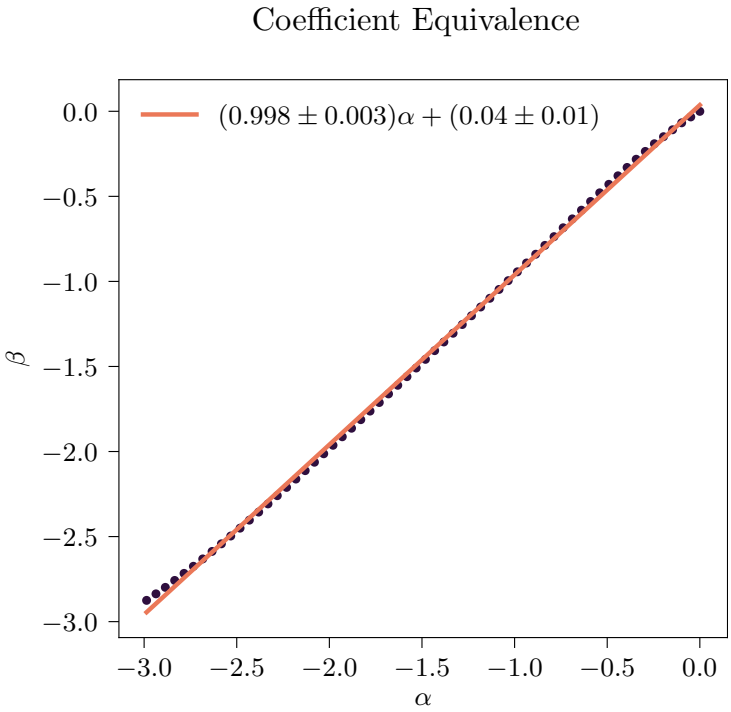

Source: Produced by the author.

For an isotropic system it can be shown that:

$$\langle \mathbf{v}^{\perp}(\mathbf{r})\mathbf{v}^{\perp *}(\mathbf{r}')\rangle = \int \langle |\tilde{\mathbf{v}}^{\perp}(\mathbf{k})|^2\rangle e^{\mathbf{k}\cdot(\mathbf{r}-\mathbf{r}')} d^3k, \tag{4.5}$$

then, the incompressible kinetic energy per unit mass of the fluid is given by:

$$E = \frac{1}{2}\langle \mathbf{v}^{\perp}(\mathbf{r})\mathbf{v}^{\perp *}(\mathbf{r})\rangle = \frac{1}{2}\int \langle |\tilde{\mathbf{v}}^{\perp}(\mathbf{k})|^2\rangle d^3k = \int \mathcal{E}(k) d^3k. \tag{4.6}$$

To obtain the spectrum, $\mathcal{E}_k$, we need to evaluate the quantity, $\langle |\tilde{\mathbf{v}}^{\perp}(\mathbf{k})|^2\rangle$, and as we previously mentioned this is quite difficult to do in general due to the nature of the velocity field. We will demonstrate that by using the fact that $\mathbf{v}^{\perp} = \frac{\pi}{2}\mathbf{v}_{\phi}^{\perp} \propto \mathbf{j}_{\phi}^{\perp}$, then it becomes straightforward.

From Eq. (4.6) we can start evaluating the spectrum by making use of the auxiliary wavefunction. We can obtain the incompressible part of a vector field in $k-$space in a general way by using the following relationship

$$\mathbf{B}^{\perp} = (\mathbf{I} - \frac{\mathbf{kk}}{|\mathbf{k}|^2}) \cdot \mathbf{B}, \tag{4.7}$$

Figure 4.4: Direct comparison of the wave spectrum and density profiles of the original wavefunction ψ and auxiliary wavefunction ϕ for the special case of $\alpha = -3$.

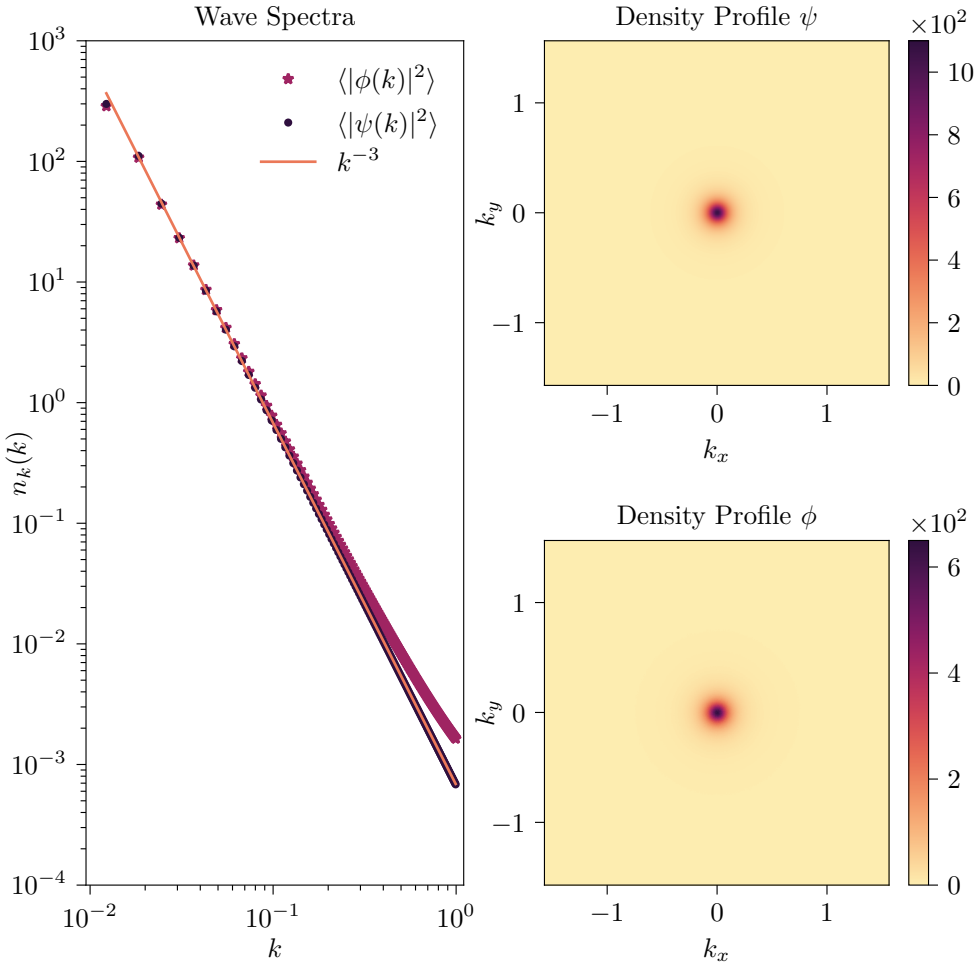

Source: Produced by the author.

with $\mathbf{I}$ being the identity tensor and $\mathbf{B}$ a generic vector field. We also note that

$$\mathbf{v}^{\perp} = \frac{\pi}{2}\mathbf{v}_{\phi}^{\perp} = \mathbf{j}_{\phi}^{\perp} \implies \mathcal{E}(k) = \frac{1}{2}\left\langle \tilde{\mathbf{j}}_{\tilde{\phi}}^{\perp}(\mathbf{k})\tilde{\mathbf{j}}_{\tilde{\phi}}^{\perp *}(\mathbf{k}')\right\rangle \delta\left(\mathbf{k}-\mathbf{k}'\right), \tag{4.8}$$

so calculating the correlation of the particle current of the auxiliary wavefunction is mathematically identical to calculating the same quantity for the velocity field of the original wavefunction. To evaluate (4.8) we start by writing $\tilde{\mathbf{j}}_{\phi}$ as a function of the Fourier transform of the auxiliary wavefunction ϕ,

$$\tilde{\mathbf{j}}_{\phi}(\mathbf{k}) = \frac{1}{(2\pi)^3}\int \left(2\mathbf{k}_1 - \mathbf{k}\right)\tilde{\phi}(\mathbf{k}_1)\tilde{\phi}^*(\mathbf{k}_1 - \mathbf{k})dk_1^3, \tag{4.9}$$

which is done by replacing directly the Fourier representation of ϕ into the definition of the

particle current, then

$$\begin{aligned}\tilde{\mathbf{j}}_{\phi}^{\perp}(\mathbf{k}) &= (\mathbb{I} - \frac{\mathbf{kk}}{|k|^2}) \cdot \tilde{\mathbf{j}}_{\phi}(\mathbf{k}) \\ bb &= \frac{1}{(2\pi)^3} \int \left[2\mathbf{k}_1 - 2 \left(\frac{\mathbf{k} \cdot \mathbf{k}_1}{|\mathbf{k}|^2} \right) \mathbf{k} \right] \tilde{\phi}(\mathbf{k}_1) \tilde{\phi}^*(\mathbf{k}_1 - \mathbf{k}) dk_1^3,\end{aligned} \tag{4.10}$$

gives us the incompressible part of the particle current which in turn leads to

$$\begin{aligned}\mathcal{E}_{\phi}(k) &= \frac{1}{2} \left\langle |\tilde{\mathbf{j}}_{\phi}^{\perp}(\mathbf{k})|^2 \right\rangle \delta(\mathbf{k} - \mathbf{k}') \\ &= \frac{\delta(\mathbf{k} - \mathbf{k}')}{2(2\pi)^6} \int dk_1^3 |\mathbf{M}(\mathbf{k}, \mathbf{k}_1)|^2 n(\mathbf{k}_1) n(\mathbf{k}_1 - \mathbf{k}),\end{aligned} \tag{4.11}$$

with $\mathbb{I}$ representing the identity tensor,

$$\mathbf{M}(\mathbf{u}, \mathbf{w}) = 2\mathbf{w} - 2 \left(\frac{\mathbf{u} \cdot \mathbf{w}}{|\mathbf{u}|^2} \right) \mathbf{u}, \tag{4.12}$$

and we used the WWT to solve the auxiliary wavefunction correlators in terms of $n(\mathbf{k})$.

Since $n(\mathbf{k}) = \mathcal{A}_k k^{\alpha}$, where $\mathcal{A}_k$ is a proportionality constant dependent on the system initial conditions, we can write (4.11) as:

$$\mathcal{E}_{\phi}(k) = \frac{\delta(\mathbf{k} - \mathbf{k}')}{2(2\pi)^6} \int dk_1 W(k, k_1), \tag{4.13}$$

with

$$W(k, k_1) = k_1^{\alpha+4} \int \mathrm{d}\Omega \, (k_1^2 - 2k_1 k \cos\theta + k^2)^{\alpha/2} \sin^2\theta,$$

$$\mathrm{d}\Omega = \sin\theta \, \mathrm{d}\theta \, \mathrm{d}\varphi \,, \quad \varphi \in [0, 2\pi), \quad \theta \in [0, \pi)$$

Using the isotropy and homogeneity of the system and a change of variables

$$\begin{aligned} k_1 &\to kx \\ \mathrm{d}k_1 &\to k \, \mathrm{d}x \\ W(k, k_1) &\to k^{2\alpha+5} W(1, x)\end{aligned} \tag{4.14}$$

leads to

$$\mathcal{E}_{\phi}(k) = \frac{\delta(\mathbf{k} - \mathbf{k}')}{2(2\pi)^5} \mathcal{A}_k^2 k^{2\alpha+5} \int_{K_-/k}^{K_+/k} W(x) dx \tag{4.15}$$

$$W(x) = x^{4+\alpha} \int_0^{\pi} (x^2 + 2x\cos\theta + 1)^{\frac{\alpha}{2}} \sin^3(\theta) d\theta \tag{4.16}$$

The limits $K_\pm$ represent the boundary of the inertial range in which the cascading solutions, from the WWT, are valid. Then one can obtain the asymptotic behaviour by expanding $W(x)$ in the limits $k \ll K_+$ and $k \gg K_-$ and solving the integral up to leading order in k.

For example, the leading behaviour of $W(x)$ as $x \to \frac{K_+}{k}$ is given by

$$\left(x^2 + 2x\cos\theta + 1\right)^{\alpha/2} \sim x^\alpha \Rightarrow W(x) \sim x^{2\alpha+4}$$

and the convergence of the integral depends on the possible values of α, in this particular full convergence of the integral is only possible if $2\alpha + 5 < 0$. If $2\alpha + 5 = 0$ the system will be logarithmically divergent and if $2\alpha + 5 > 0$ it will have an ultraviolet divergence proportional to the K_+ boundary.

The solutions are then heavily dependent on the value of the power-law coefficient α, Eq. (4.17) summarizes the different cases based both on the leading behaviours and the possible values of α.

$$\mathcal{E}(k) \sim \begin{cases} k^\alpha, & \text{if } \alpha < -5, \\ k^{-5}\log(k), & \text{if } \alpha = -5, \\ k^{2\alpha+5}, & \text{if } -5 < \alpha < -\frac{5}{2}, \\ \log\left(\frac{1}{k}\right), & \text{if } \alpha = -\frac{5}{2}, \\ k^0, & \text{if } \alpha > -\frac{5}{2}, \end{cases} \tag{4.17}$$

In the literature it is typical to discuss the energy spectrum in terms of the $1D$ spectrum given as $\mathcal{E}^{(1D)}(k) = 4\pi k^2 \mathcal{E}(k)$. This is done by considering the isotropy of the system and integrating out the solid angle in the last term of Eq. (4.6):

$$\int \mathcal{E}(\mathbf{k}) d^3k = \int 4\pi k^2 \mathcal{E}(k) dk = \int \mathcal{E}^{(1D)}(k) dk.$$

Therefore, Eq. (4.17) can be written as

$$\mathcal{E}^{(1D)}(k) \sim \begin{cases} k^{\alpha+2}, & \text{if } \alpha < -5, \\ k^{-3}\log(k), & \text{if } \alpha = -5, \\ k^{2\alpha+7}, & \text{if } -5 < \alpha < -\frac{5}{2}, \\ k^2\log\left(\frac{1}{k}\right), & \text{if } \alpha = -\frac{5}{2}, \\ k^2, & \text{if } \alpha > -\frac{5}{2}. \end{cases} \tag{4.18}$$

4.4 Further Discussion

The spectra obtained in (4.18) are all dependent on the coefficient, α, but only a subset of values is physically relevant. The WWT theory, in the $3D$ case, offers two cascading solutions

for the kinetic equation, a waveaction cascade with $\alpha = -\frac{7}{3}$ and an energy cascade with $\alpha = -3$. Aside from these two solutions there is also the critical balance conjecture, which considers the system when the interaction and kinetic energy are comparable, such situation was observed by Proment, Nazarenko, and Onorato [62] with $n(k) \sim k^{-4}$. With these values we see that the physically relevant results from Eq. (4.18) are:

$$\mathcal{E}^{(1D)}(k) \sim \begin{cases} k^{2\alpha+7}, & \text{if } -5 < \alpha < -\frac{5}{2}, \\ k^2, & \text{if } \alpha > -\frac{5}{2}, \end{cases} \tag{4.19}$$

The predicted WWT spectra $\mathcal{E}^{(1D)}_{WT} \sim k^{\alpha+4}$ also coincides with the one obtained by our method $\mathcal{E}^{(1D)}(k) \sim k^{2\alpha+7}$ for the energy cascade solution, which seems to be coincidental since the WWT energy spectra prediction represents the sum of compressible plus incompressible spectra.

The results predicted by the use of the auxiliary wavefunction can be verified by numerically averaging the velocity field correlator and calculating the spectrum in Fourier representation. Figures 4.5 and 4.6 shows the incompressible energy spectrum for $\psi \sim k^{-\frac{3}{2}}$ and $\psi \sim k^{-2}$. A linear regression showing the best fit approximation is included in both figures. The numerically obtained coefficients shows agreement with the ones extracted from (4.19) for $\alpha = -3$ and $\alpha = -4$.

Figure 4.5: Incompressible kinetic energy spectrum, calculated for $\psi \sim k^{-\frac{3}{2}}$, and best fit (straight line) approximation.

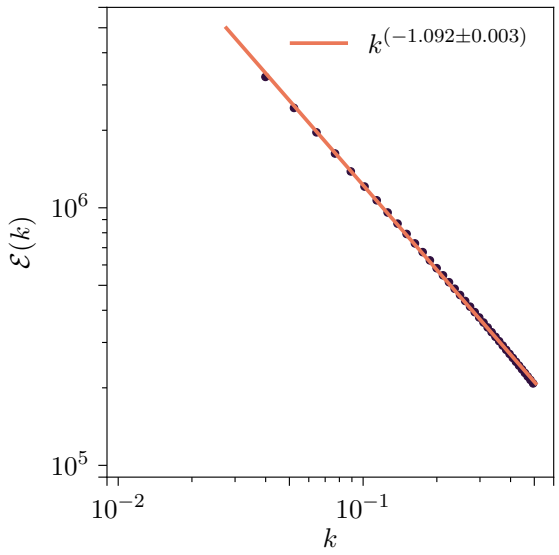

The spectrum of Fig. 4.6, $\mathcal{E}^{(1D)}(k) \sim k^{-0.898}$, obtained for $\alpha = -4$ is related to the wave spectrum of the critical balance conjecture and is comparable to the incompressible energy

Figure 4.6: Incompressible kinetic energy spectrum, calculated for $\psi \sim k^{-2}$, and best fit (straight line) approximation.

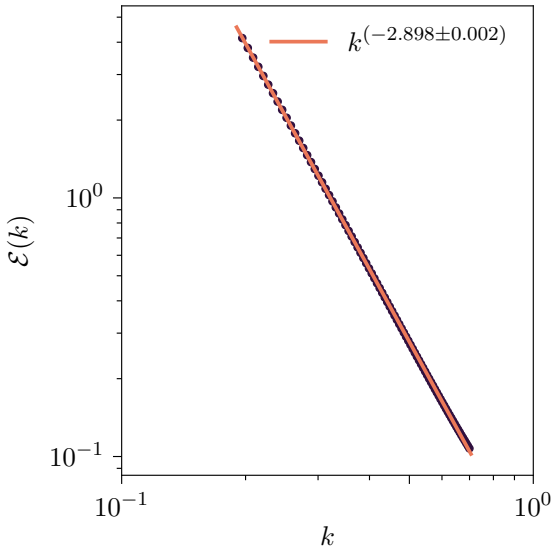

spectrum observed in Proment, Nazarenko, and Onorato [62, see Fig. 21] near the critical balance regime. We showed that this spectrum comes from the velocity field statistics as a consequence of the wave spectrum and, since it happens in the transition from the 4-wave to 3-wave regime, it could indicate the manifestation of Vinen type turbulence in the transition process, but more investigation would be needed particularly in the vortex decay near the 4-wave to 3-wave transition.

It should be noted that the plots in Fig. 4.5 and Fig. 4.6 were obtained by preparing a wave function with the characteristics of a WWT solution, in this case the energy cascade and critical balance conjecture, respectively. After preparing the wavefunction we calculated the velocity field and used the Helmholtz decomposition to obtain its incompressible part and calculated the autocorrelation, a multiple sample average was used to reduce the noise from the random phase field. To finally obtain the spectrum we used a radial average to integrate out the solid angle, followed by the best fit analysis to numerically calculate the angular coefficient.

4.5 Final Remarks

In summary, we demonstrated that there is a direct relationship between the Kolmogorov–Zakharov power law cascades from wave turbulence and the statistics of the incompressible velocity field of an atomic BEC. That was done by analytically calculating an analogue to the classical K41 spectrum directly from the statistical distribution of the velocity field, which

was possible by using an auxiliary wavefunction that not only evades the discontinuities of the velocity field but also reproduces the statistical properties of the GPE wavefunction. The result obtained not only demonstrates a link between wave turbulence and hydrodynamic turbulence but presents, as far as the author knows, the first analytical calculation of the velocity field distribution spectrum for atomic BEC.

The possible connection with Vinen turbulence is the most interesting result since it offers a theoretical explanation to the numerically observed k^{-1} spectrum of previously numerical simulations of WWT. It is also interesting to note that recent [54] numerical investigations of Vinen turbulence in atomic BEC observed possible signs of a wave turbulence happening simultaneously. This could mean that the accumulation of particles in the ground state characteristic of WWT could serve as a driving mechanism for Vinen type turbulence. To further investigate this possibility careful numerical investigations must be done with particular focus on the vortex line decay and both the wave spectrum and incompressible energy spectrum near the transition from 4-wave WWT to 3-wave WWT. Another consideration for future explorations is a more formal interpretation on the relationship of the auxiliary wavefunction with the wave statistics without needing to rely on numerics.

Bibliography

[1] P. Kapitza. "Viscosity of Liquid Helium below the λ-Point." en. In: *Nature* 141 (3558 Jan. 1938), pp. 74–74. DOI: 10.1038/141074a0 (cit. on p. 1).

[2] J. F. Allen and A. D. Misener. "Flow of Liquid Helium II." en. In: *Nature* 141.3558 (3558 Jan. 1938), pp. 75–75. ISSN: 0028-0836, 1476-4687. DOI: 10.1038/141075a0 (cit. on p. 1).

[3] Seth J. Putterman and Isadore Rudnick. "Quantum nature of superfluid helium." en. In: *Physics Today* 24 (8 Aug. 1971), pp. 39–47. DOI: 10.1063/1.3022882 (cit. on p. 1).

[4] W.H. Keesom and G.E. Macwood. "The viscosity of liquid helium." en. In: *Physica* 5 (8 Aug. 1938), pp. 737–744. DOI: 10.1016/s0031-8914(38)80195-6 (cit. on p. 1).

[5] L. Tisza. "Transport Phenomena in Helium II." en. In: *Nature* 141.3577 (3577 May 1938), pp. 913–913. ISSN: 0028-0836, 1476-4687. DOI: 10.1038/141913a0 (cit. on p. 1).

[6] L. Landau. "Theory of the Superfluidity of Helium II." en. In: *Physical Review* 60 (4 Aug. 1941), pp. 356–358. DOI: 10.1103/physrev.60.356 (cit. on p. 1).

[7] F. London. "The λ-Phenomenon of Liquid Helium and the Bose-Einstein Degeneracy." en. In: *Nature* 141.3571 (3571 Apr. 1938), pp. 643–644. ISSN: 0028-0836, 1476-4687. DOI: 10.1038/141643a0 (cit. on p. 1).

[8] R.P. Feynman. "Chapter II Application of Quantum Mechanics to Liquid Helium." en. In: *Helium 4*. Elsevier, 1955, pp. 17–53. ISBN: 978-0-08-015816-7. DOI: 10.1016/s0079-6417(08)60077-3 (cit. on p. 1).

[9] L. Onsager. "Statistical hydrodynamics." en. In: *Il Nuovo Cimento* 6 (S2 Mar. 1949), pp. 279–287. DOI: 10.1007/bf02780991 (cit. on p. 1).

[10] Oliver Penrose and Lars Onsager. "Bose-Einstein Condensation and Liquid Helium." en. In: *Physical Review* 104.3 (3 Nov. 1956), pp. 576–584. DOI: 10.1103/physrev.104.576 (cit. on p. 1).

[11] W. F. Vinen. "Detection of Single Quanta of Circulation in Rotating Helium II." en. In: *Nature* 181.4622 (4622 May 1958), pp. 1524–1525. ISSN: 0028-0836, 1476-4687. DOI: 10.1038/1811524a0 (cit. on p. 1).

[12] A. Einstein. *Quantentheorie des einatomigen idealen Gases*. Dec. 2005. DOI: 10.1002/3527608958.ch27 (cit. on p. 1).

[13] Albert Einstein et al. *Collected Papers of Albert Einstein Vol. 14 - The Berlin Years - Writings and Correspondence, April 1923-May 1925*. Princeton University Press, 2014. ISBN: 9780691164229 (cit. on p. 2).

[14] N. Bogolubov. "On The Theory Of Superfluidity." In: *Helium 4* (1971), pp. 247–267. DOI: 10.1016/b978-0-08-015816-7.50020-1 (cit. on p. 2).

[15] E. P. Gross. "Structure of a quantized vortex in boson systems." en. In: *Il Nuovo Cimento* 20 (3 May 1961), pp. 454–477. DOI: 10.1007/bf02731494 (cit. on pp. 2, 9).

[16] LP Pitaevskii. "Vortex Lines in an Imperfect Bose Gas." In: *Sov. Phys. JETP* 13.2 (1961), pp. 451–454 (cit. on pp. 2, 9).

[17] M. H. Anderson et al. "Observation of Bose-Einstein Condensation in a Dilute Atomic Vapor." en. In: *Science* 269.5221 (5221 July 1995), pp. 198–201. DOI: 10.1126/science.269.5221.198 (cit. on pp. 2, 5).

[18] K. B. Davis et al. "Bose-Einstein Condensation in a Gas of Sodium Atoms." en. In: *Physical Review Letters* 75 (22 Nov. 1995), pp. 3969–3973. DOI: 10.1103/physrevlett.75.3969 (cit. on pp. 2, 5).

[19] M. R. Matthews et al. "Vortices in a Bose-Einstein Condensate." en. In: *Physical Review Letters* 83.13 (13 Sept. 1999), pp. 2498–2501. DOI: 10.1103/physrevlett.83.2498 (cit. on p. 2).

[20] C. Raman et al. "Vortex Nucleation in a Stirred Bose-Einstein Condensate." en. In: *Physical Review Letters* 87 (21 Nov. 2001). DOI: 10.1103/physrevlett.87.210402 (cit. on p. 2).

[21] E. A. L. Henn et al. "Observation of vortex formation in an oscillating trapped Bose-Einstein condensate." en. In: *Physical Review A* 79.4 (4 Apr. 2009), p. 043618. ISSN: 1050-2947, 1094-1622. DOI: 10.1103/physreva.79.043618 (cit. on pp. 2, 21).

[22] Yoshio Torii et al. "Mach-Zehnder Bragg interferometer for a Bose-Einstein condensate." en. In: *Physical Review A* 61 (4 Feb. 2000). DOI: 10.1103/physreva.61.041602 (cit. on p. 2).

[23] Jean Macher and Renaud Parentani. "Black-hole radiation in Bose-Einstein condensates." en. In: *Physical Review A* 80 (4 Oct. 2009). DOI: 10.1103/physreva.80.043601 (cit. on p. 2).

[24] David C. Aveline et al. "Observation of Bose–Einstein condensates in an Earth-orbiting research lab." en. In: *Nature* 582 (7811 June 2020), pp. 193–197. DOI: 10.1038/s41586-020-2346-1 (cit. on p. 2).

[25] U. Frisch. *Turbulence - the legacy of A.N. Kolmogorov*. Cambridge University Press, 1995. ISBN: 9780521457132 (cit. on pp. 2, 15).

[26] J Maurer and P Tabeling. "Local investigation of superfluid turbulence." In: *Europhysics Letters (EPL)* 43 (1 July 1998), pp. 29–34. DOI: 10.1209/epl/i1998-00314-9 (cit. on p. 2).

[27] E. A. L. Henn et al. "Emergence of Turbulence in an Oscillating Bose-Einstein Condensate." en. In: *Physical Review Letters* 103.4 (4 July 2009), p. 045301. ISSN: 0031-9007, 1079-7114. DOI: 10.1103/physrevlett.103.045301 (cit. on pp. 2, 21).

[28] Tsubota Makoto. *Quantum Turbulence*. Elsevier, 2009. ISBN: 9780080548104. DOI: 10.1016/s0079-6417(08)x0001-0 (cit. on pp. 2, 21).

[29] Marios C. Tsatsos et al. "Quantum turbulence in trapped atomic Bose–Einstein condensates." en. In: *Physics Reports* 622 (Mar. 2016), pp. 1–52. DOI: 10.1016/j.physrep.2016.02.003 (cit. on pp. 2, 21).

[30] L. Madeira et al. "Quantum turbulence in Bose–Einstein condensates: Present status and new challenges ahead." en. In: *AVS Quantum Science* 2 (3 Oct. 2020), p. 035901. DOI: 10.1116/5.0016751 (cit. on pp. 2, 21).

[31] Sergey Nazarenko. "Wave turbulence." en. In: *Contemporary Physics* 56 (3 July 2015), pp. 359–373. DOI: 10.1080/00107514.2015.1015250 (cit. on p. 2).

[32] V. S. L'vov and S. Nazarenko. "Spectrum of Kelvin-wave turbulence in superfluids." en. In: *JETP Letters* 91.8 (8 Apr. 2010), pp. 428–434. ISSN: 0021-3640, 1090-6487. arXiv: 0911.2065. DOI: 10.1134/s002136401008014x (cit. on p. 2).

[33] Charles Kittel. *Thermal physics*. W. H. Freeman, 1980. ISBN: 9780716710882 (cit. on p. 5).

[34] C. J. Pethick and H. Smith. *Bose–Einstein Condensation in Dilute Gases*. Cambridge University Press, 2008. ISBN: 9780511802850. DOI: 10.1017/cbo9780511802850 (cit. on pp. 6, 11, 17).

[35] V. I. Yukalov. "Basics of Bose-Einstein condensation." en. In: *Physics of Particles and Nuclei* 42 (3 May 2011), pp. 460–513. DOI: 10.1134/s1063779611030063 (cit. on pp. 6, 11).

[36] Allan Griffin, D. W. Snoke, and S. Stringari. *Bose-Einstein condensation*. Cambridge University Press, 1995. ISBN: 9780521464734 (cit. on p. 11).

[37] Carlo Barenghi and Nick G. Parker. *A Primer on Quantum Fluids*. Springer International Publishing, 2016. ISBN: 9783319424767. DOI: 10.1007/978-3-319-42476-7 (cit. on p. 11).

[38] Richard Phillips Feynman, Robert B. Leighton, and Matthew Sands. *The Feynman Lectures on Physics, Vol. II: The New Millennium Edition: Mainly Electromagnetism and Matter*. Basic Books, 2011. ISBN: 9780465024940 (cit. on p. 14).

[39] Lev Davidovich Landau. *Fluid mechanics*. Pergamon Press, 1987. ISBN: 9780080339337 (cit. on p. 14).

[40] Lewis F. Richardson. "Atmospheric diffusion shown on a distance-neighbour graph." en. In: *Proceedings of the Royal Society of London. Series A, Containing Papers of a Mathematical and Physical Character* 110.756 (756 Apr. 1926), pp. 709–737. DOI: 10.1098/rspa.1926.0043 (cit. on p. 15).

[41] D. C. Leslie. *Developments in the theory of turbulence*. Clarendon Press, 1973. ISBN: 9780198563181 (cit. on p. 15).

[42] W. D. McComb. *The physics of fluid turbulence*. Clarendon Press, 1991. ISBN: 9780198562566 (cit. on p. 15).

[43] A. N. Kolmogorov. "The local structure of turbulence in incompressible viscous fluid for very large Reynolds numbers." en. In: *Proceedings of the Royal Society of London. Series A: Mathematical and Physical Sciences* 434.1890 (1890 July 1991), pp. 9–13. ISSN: 0962-8444, 2053-9177. DOI: 10.1098/rspa.1991.0075 (cit. on p. 15).

[44] G. K. Batchelor. *The theory of homogeneous turbulence*. Cambridge University Press, 1982. ISBN: 9780521041171 (cit. on p. 15).

[45] F. Ednilson A. dos Santos. "Hydrodynamics of vortices in Bose-Einstein condensates: A defect-gauge field approach." en. In: *Physical Review A* 94.6 (6 Dec. 2016). ISSN: 2469-9926, 2469-9934. DOI: 10.1103/physreva.94.063633 (cit. on pp. 17, 18, 20, 33).

[46] Michikazu Kobayashi and Makoto Tsubota. "Kolmogorov Spectrum of Superfluid Turbulence: Numerical Analysis of the Gross-Pitaevskii Equation with a Small-Scale Dissipation." en. In: *Physical Review Letters* 94.6 (6 Feb. 2005), p. 065302. DOI: 10.1103/physrevlett.94.065302 (cit. on p. 20).

[47] C. Nore, M. Abid, and M. E. Brachet. "Kolmogorov Turbulence in Low-Temperature Superflows." en. In: *Physical Review Letters* 78.20 (20 May 1997), pp. 3896–3899. ISSN: 0031-9007, 1079-7114. DOI: 10.1103/physrevlett.78.3896 (cit. on p. 20).

[48] Ashton S. Bradley and Brian P. Anderson. "Energy Spectra of Vortex Distributions in Two-Dimensional Quantum Turbulence." en. In: *Physical Review X* 2 (4 Oct. 2012). DOI: 10.1103/physrevx.2.041001 (cit. on p. 20).

[49] A. Cidrim et al. "Vinen turbulence via the decay of multicharged vortices in trapped atomic Bose-Einstein condensates." en. In: *Physical Review A* 96 (2 Aug. 2017). DOI: 10.1103/physreva.96.023617 (cit. on p. 20).

[50] G. E. Volovik. "Classical and quantum regimes of superfluid turbulence." en. In: *Journal of Experimental and Theoretical Physics Letters* 78 (9 Nov. 2003), pp. 533–537. DOI: 10.1134/1.1641478 (cit. on p. 20).

[51] L. Skrbek. "A flow phase diagram for helium superfluids." en. In: *Journal of Experimental and Theoretical Physics Letters* 80 (7 Oct. 2004), pp. 474–478. DOI: 10.1134/1.1839293 (cit. on p. 20).

[52] Makoto Tsubota. "Quantum Turbulence." en. In: *Journal of the Physical Society of Japan* 77.11 (11 Nov. 2008), p. 111006. ISSN: 0031-9015, 1347-4073. DOI: 10.1143/jpsj.77.111006 (cit. on p. 20).

[53] Michikazu Kobayashi and Makoto Tsubota. "Kolmogorov Spectrum of Quantum Turbulence." en. In: *Journal of the Physical Society of Japan* 74 (12 Dec. 2005), pp. 3248–3258. DOI: 10.1143/jpsj.74.3248 (cit. on p. 20).

[54] Áttis V. M. Marino et al. "Momentum distribution of Vinen turbulence in trapped atomic Bose–Einstein condensates." en. In: *The European Physical Journal Special Topics* 230 (4 June 2021), pp. 809–812. DOI: 10.1140/epjs/s11734-021-00083-3 (cit. on pp. 20, 43).

[55] C. F. Barenghi, Y. A. Sergeev, and A. W. Baggaley. "Regimes of turbulence without an energy cascade." en. In: *Scientific Reports* 6 (1 Dec. 2016). DOI: 10.1038/srep35701 (cit. on p. 20).

[56] A. W. Baggaley, C. F. Barenghi, and Y. A. Sergeev. "Quasiclassical and ultraquantum decay of superfluid turbulence." en. In: *Physical Review B* 85 (6 Feb. 2012). DOI: 10.1103/physrevb.85.060501 (cit. on p. 20).

[57] Vladimir E. Zakharov, Victor S. L'vov, and Gregory Falkovich. *Kolmogorov Spectra of Turbulence I*. Ed. by F. Calogero et al. Springer Series in Nonlinear Dynamics. Berlin, Heidelberg: Springer Berlin Heidelberg, 1992. ISBN: 9783642500541. DOI: 10.1007/978-3-642-50052-7 (cit. on pp. 21, 30).

[58] Sergey Nazarenko. *Wave Turbulence*. Vol. 825. Lecture Notes in Physics. Berlin, Heidelberg: Springer Berlin Heidelberg, 2011. ISBN: 9783642159411. DOI: 10.1007/978-3-642-15942-8 (cit. on pp. 21, 23–25, 31).

[59] K J Thompson et al. "Evidence of power law behavior in the momentum distribution of a turbulent trapped Bose–Einstein condensate." In: *Laser Physics Letters* 11 (1 Jan. 2014), p. 015501. DOI: 10.1088/1612-2011/11/1/015501 (cit. on p. 30).

[60] Nir Navon et al. “Emergence of a turbulent cascade in a quantum gas.” en. In: *Nature* 539 (7627 Nov. 2016), pp. 72–75. DOI: 10.1038/nature20114 (cit. on p. 30).

[61] Nir Navon et al. “Synthetic dissipation and cascade fluxes in a turbulent quantum gas.” en. In: *Science* 366 (6463 Oct. 2019), pp. 382–385. DOI: 10.1126/science.aau6103 (cit. on p. 30).

[62] Davide Proment, Sergey Nazarenko, and Miguel Onorato. “Sustained turbulence in the three-dimensional Gross–Pitaevskii model.” en. In: *Physica D: Nonlinear Phenomena* 241.3 (3 Feb. 2012), pp. 304–314. DOI: 10.1016/j.physd.2011.06.007 (cit. on pp. 30, 31, 41, 42).

[63] Davide Proment, Sergey Nazarenko, and Miguel Onorato. “Quantum turbulence cascades in the Gross-Pitaevskii model.” en. In: *Physical Review A* 80 (5 Nov. 2009). eprint: 0905.3263v1. DOI: 10.1103/physreva.80.051603 (cit. on p. 30).

[64] Kazuya Fujimoto and Makoto Tsubota. “Bogoliubov-wave turbulence in Bose-Einstein condensates.” en. In: *Physical Review A* 91 (5 May 2015). DOI: 10.1103/physreva.91.053620 (cit. on p. 31).